AFCRL-66-497
Scientific Report 2

June 1966

ROCKET MOTOR CHARGING EXPERIMENTS

By: E. F. VANCE J. E. NANEVICZ

Prepared for:

AIR FORCE CAMBRIDGE RESEARCH LABORATORIES
OFFICE OF AEROSPACE RESEARCH
UNITED STATES AIR FORCE
BEDFORD, MASSACHUSETTS

CONTRACT AF 19(628)-4800
PROJECT NO. 4600
TASK NO. 460001

STANFORD RESEARCH INSTITUTE
MENLO PARK, CALIFORNIA

*SRI

STANFORD RESEARCH INSTITUTE
MENLO PARK, CALIFORNIA

AFCRL-66-497
Scientific Report 2

June 1966

ROCKET MOTOR CHARGING EXPERIMENTS

Prepared for:

AIR FORCE CAMBRIDGE RESEARCH LABORATORIES
OFFICE OF AEROSPACE RESEARCH
UNITED STATES AIR FORCE
BEDFORD, MASSACHUSETTS

CONTRACT AF 19(628)-4800
PROJECT NO. 4600
TASK NO. 460001

By: E. F. VANCE J. E. NANEVICZ

SRI Project 5359

Approved: TETSU MORITA, MANAGER
ELECTROMAGNETIC SCIENCES LABORATORY

D. R. SCHEUCH, EXECUTIVE DIRECTOR
ELECTRONICS AND RADIO SCIENCES

FOREWORD

This report was prepared by Stanford Research Institute (SRI), Menlo Park, California, and is the second in a series of Scientific Reports issued under Air Force Contract AF 19(628)-4800, Project No. 4600, Task No. 460001. The work was administered under the Office of Aerospace Research of the Air Force Cambridge Research Laboratories. Mr. Charles Ellis was the Air Force task engineer.

The report presents the results of a study of a particular topic in the general area of problems associated with the radiation and reception of electromagnetic energy from aircraft and guided missiles. The principle investigator, Dr. J. E. Nanevicz, was responsible for research activity under Stanford Research Institute Project 5359.

Scientific Reports Issued in This Series

Scientific Report 1

"An Experimental Study of Non-Linear Plasma-Wave Interaction," by W. C. Taylor, AFCRL-65-654 (August 1965).

Scientific Report 2

"Rocket Motor Charging Experiments," by E. F. Vance and J. E. Nanevicz, AFCRL-66-497 (June 1966).

ABSTRACT

A study of the effect of rocket engines on electrostatic charge accumulation was made. Experiments were conducted to measure short-circuit charging current and open-circuit voltage produced by 5-inch solid-fuel rocket motors during static firings at sea level. Experiments were also performed with an ethylene-oxygen burner at reduced pressures (14 mmHg). The results of these experiments are presented and compared to the published results of related experiments.

Two Nike-Cajun sounding rockets were equipped with electric field meters to measure the vehicle potential throughout the rocket flight. The field meters indicated that the maximum vehicle potential was 26-to-40 kilovolts during first-stage burning at about 3 kilometers and about 2 kilovolts during second-stage burning at about 12 kilometers. At high altitudes, the field meter on the first Nike-Cajun responded to ionization present in the ionosphere and enhanced by a primary experiment. This undesired response was successfully separated from the true field response in the field meter system designed for the second Nike-Cajun experiment. It was, therefore, possible to conclude that the potential of the second vehicle was less than 1 kilovolt at altitudes above 60 kilometers (in the ionosphere).

CONTENTS

ILLUSTRATIONS

ILLUSTRATIONS (Concluded)

TABLES

I INTRODUCTION

A. The Engine Charging Phenomenon

In precipitation static studies on jet aircraft, it was observed that each take-off was accompanied by light to moderate charging regardless of the local weather conditions.[1*] A typical discharge current trace during take-off in a DC-8 aircraft is shown in Fig. 1. Since

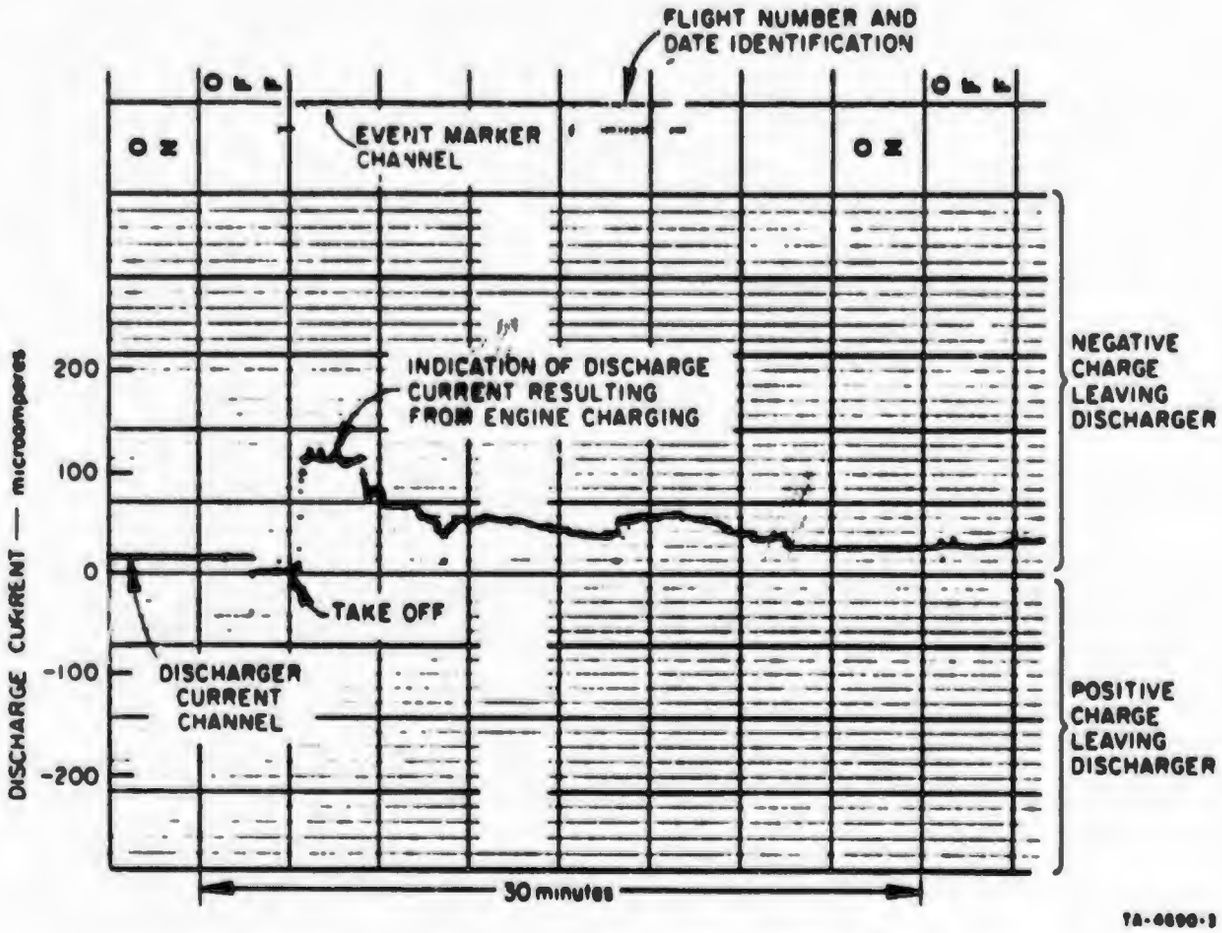

FIG. 1 TYPICAL JET ENGINE CHARGING CHARACTERISTIC FROM A DC-8 AIRCRAFT

---

* Numbered references are listed on pages 95 and 96.

fluctuations in this charging correlated with changes in throttle setting, the charging was attributed to the jet engines. Furthermore, it was noticed that on aircraft equipped with water injection systems, the engine charging rate increased by a factor of 3 to 5 during water injection, returning to the normal "dry" level when the water was expended. After take-off, engine charging gradually decreased until, at cruise altitude, it reached a level of 1 to 5 μamp which continued throughout the flight. Since the maximum engine charging rate observed was about 800 μamp (for all four engines with water injection), whereas maximum precipitation charging rates of the order of 5 mamp had been observed, engine charging on jet aircraft was not considered an important problem.

It has been suggested that engine charging is a result of plasma processes within the combustion chamber.[2] This hypothesis proposes that within the thermally ionized combustion products, the electrons, being more mobile that the positive ions, diffuse to the combustion chamber walls leaving a positive ion sheath adjacent to the walls. Part of this ion sheath is then expelled with the exhaust gases, leaving the motor housing negatively charged. Since the combustion chamber in a jet engine is completely enclosed in metal except at the exhaust ports, the electron charge deposited on the inside surface of the chamber immediately flows to the outside surface, leaving only the sheath field within the chamber. Thus further diffusion of electrons to the walls is not inhibited by the charge already acquired by the walls (and distributed over the outside surface of the chamber). In other words, the sheath structure within the chamber is not affected by the net charge on the vehicle. By the time the exhaust gas reaches the exit, the gas has expanded and cooled, and the electrons have attached to form less mobile negative ions. Both the positive ions and the negative ions in the exhaust have such low mobilities that most of them are carried away by the wind stream even when the aircraft is charged to a potential of several hundred kilovolts.

This explanation of the engine charging mechanism seemed to be consistent with the following characteristics of jet engine charging:

(1) The engines always charge the aircraft negatively (electron collection).

(2) The charging rate depends on the engine power setting (combustion chamber temperature) and altitude (ion mobility).

(3) The mobility and concentration of ions in the exhaust were too low at sea level to discharge aircraft through the exhaust. (A high voltage probe in the exhaust stream failed to collect appreciable current of either polarity.)

As indicated above, engine charging on aircraft was of secondary interest, because precipitation charging rates were much greater than engine charging rates. It was postulated that engine charging on rocket vehicles might be of primary interest, however, since rocket engines are larger in relation to the vehicle than are aircraft engines. Furthermore, combustion chamber temperatures and electron densities are higher in rocket engines than in jet engines, and vehicle velocities are greater. In addition to these factors, which would tend to make rocket engine charging more severe, it was thought that the hotter exhaust of the rocket motor might tend to limit vehicle potentials, since the electrons and ions in the exhaust would be more mobile and present in higher concentrations than in the colder jet engine exhaust.

Unfortunately, a dearth of experimental data on either the engine-charging mechanism or typical rocket motor charging rates has precluded a conclusive analysis of the rocket motor charging. Although the electron diffusion theory seemed to explain jet engine charging, at least qualitatively, several other charging mechanisms have also been proposed to explain the rocket engine charging phenomenon.[3,4,5] Some of these mechanisms lead to positive charging currents, while others lead to negative charging currents. Without corroborating experimental data, therefore, any analyses of engine charging mechanisms must be viewed as speculative.

B. The Importance of Engine Charging

Rocket vehicles that become charged to high potentials may be subject to the same interference problems that are encountered by

aircraft--namely radio frequency noise produced by corona discharges from the extremities of the vehicle, streamer discharges on insulating surfaces that become triboelectrically charged, particle impact, and spark discharges between unbonded sections. In addition, rocket vehicles often contain digital computers in their guidance and control systems which are susceptible to the impulsive interference produced by streamer and spark discharges. Rocket vehicles also use electroexplosive devices extensively for motor ignition, staging, and numerous other purposes. These devices can be prematurely ignited by discharges of static electricity, thereby degrading system performance or inducing complete failure of the mission. It has also been postulated that rendezvous and docking maneuvers may be hampered if the two vehicles participating in the maneuver are at different potentials prior to contact.

In order to determine the severity of these problems and establish techniques for alleviating the problems on rocket vehicles, it is necessary to determine the vehicle charging rates and potentials that will be encountered on typical missions. Under a separate program, the problem of triboelectric charging of high speed vehicles has been investigated.[8] Because it was postulated that engine charging might be the predominant charging mechanism on rocket vehicles, an experimental investigation of this mechanism was undertaken on the present program. Although the precise mechanism by which the engines charge the vehicle is still open for debate, the results of this experimental program provide some data by which theoretical analyses can be tested. It is anticipated that the experimental data may also help to dissipate some of the confusion that presently exists in regard to vehicle electrification.

One factor that has lent confusion to the rocket engine charging problem is the tendency to indiscriminately intermingle jet aircraft charging characteristics and rocket charging characteristics. For example, because jet engines can charge an aircraft to its corona threshold potential of about 200 kilovolts at sea level, it has been assumed that rocket engines will charge the vehicles to similar potentials at high altitudes as well as at sea level. It is probable that a

great deal of the confusion stems from the fact that only short-circuit engine charging current data (i.e., the charging current at zero engine potential) have been available to workers in this area. Since the short-circuit charging currents for rocket engines may be relatively large compared to the jet engine charging currents, some rather high potentials resulting from rocket engine charging have been predicted. In fact, however, the rocket exhaust is much more highly ionized (and therefore more conductive) than the relatively cold and poorly conducting jet engine exhaust. Thus, the rocket engine charging current is strongly dependent on the vehicle potential because of the ability of the charged vehicle to collect a neutralizing current from the conductive exhaust plume.

Because the rocket exhaust is decidedly different from the jet engine exhaust, it appears that the rocket engine will have one of three effects on the vehicle potential. First, if the engines are capable of charging the vehicle to potentials above the vehicle threshold potential (in which case the rocket engine behavior would be quite similar to that of the jet engine), corona discharges and electromagnetic interference would accompany each launch. In this case, it might be necessary to provide some method for reducing the interference produced by the corona discharge, such as is provided on aircraft.

A second possibility is that the conductivity of the exhaust is sufficient to limit the vehicle potential to some value below the threshold potential. If the vehicle potential does not exceed the corona threshold potential, there will be no corona discharges or associated electromagnetic interference (if engine charging is the only source of electrostatic charge accumulation). Spark discharges between unbonded sections would then be the primary problem associated with engine charging. Since this problem can be eliminated by adequate bonding, engine charging would probably be less serious than triboelectric charging in this case.

A third possibility is that the ionized rocket exhaust is so effective in limiting the vehicle potential that the vehicle potential is maintained below the corona threshold potential even when other charging sources, such as triboelectric charging from precipitation or dust

particles, are active. If this were the case, the rocket engine would tend to alleviate, rather than aggravate, the vehicle charging problem. As an historical note, it is pointed out that it was originally anticipated that the engines would alleviate the precipitation static problem on jet aircraft.[6] Because of the extremely low conductivity of the jet engine exhaust, however, jet engines were found to be effective aircraft chargers (i.e., the equilibrium potential of the jet engines is higher than the corona threshold potential).

C. Scope of This Study

The purpose of this study was to measure the charging currents and potentials produced by rocket engines in order that typical engine charging characteristics could be established. To obtain these charging characteristics, three series of experiments were conducted. These were: (1) a series of static firings of small solid-fuel motors in which short-circuit charging current was measured, (2) a second series of static firings in which open circuit voltages were measured, and (3) a series of instrumented flight tests in which the potentials of Nike-Cajun rockets were measured in flight. In the following sections, these experiments will be described in detail.

In general, this work served to point out the complexity of the engine charging problem. It appears that several competing mechanisms occur simultaneously, and that the polarity and magnitude of the net charging current are determined by which mechanism predominates. Although several charging mechanisms may be operating simultaneously, the experimental results reported here suggest that the conductivity of the rocket exhaust is high enough to limit the vehicle potential to values below the corona threshold potential. In addition to providing experimental data heretofore unavailable, this report indicates areas in which more refined work could profitably be done.

II STATIC FIRING TESTS

A. Short Circuit Current Measurements

A review of the state of knowledge regarding rocket motor charging indicated that virtually no experimental data were available to permit the testing and refinement of theories regarding the charging processes involved. In casting about for ways of obtaining experimental data, the possibility of performing charging measurements during static firings of rocket motor suggested itself. It was recognized at this time that many of the charging processes are markedly affected by the presence of a windstream about the rocket, and that, ideally, the measurements should be made on rocket vehicles in flight. Flight testing however, is costly, so that only a limited number of flights can ever be contemplated. Furthermore, only a limited amount of information can be obtained per flight. For example, during a given flight, it is possible to study only one fuel mixture and one nozzle configuration. In the light of these considerations it was felt that an investigation of the rocket charging problem should include measurements made during static motor firings. A measurement of short circuit charging current appeared to be a desirable first step since the measurement is relatively easy to implement, and it was argued that the short circuit current would be representative of the minimum short circuit charging current that would be obtained in flight. The charging processes occurring in the combustion chamber are unaffected by the motion of the vehicle so that the total charge expelled should be the same during the static test as it is in flight. The circulation of charge from the exhaust back to the vehicle should be higher when the vehicle is stationary than when the vehicle is moving so that the net charging current generated by a stationary motor should be less than that generated in flight.

Details of the short circuit current measurements conducted at SRI are presented in Appendix A Only a brief description of the experiment together with the results and conclusions of these measurements will be given here.

The initial short circuit charging current measurements were made on a "piggy-back" basis using a set of three 5-inch diameter solid-fuel motors containing a basic fuel consisting of polyurethane and ammonium perchlorate seeded with potassium. (For the second and third firings aluminum powder was added to the fuel.) For the basic experiment, the engine exhausted into a steel diffuser tube separated from the motor by a hard glass pipe. Provisions were made to electrically isolate both the motor and the diffuser and to measure the current flowing to ground from both the motor and the diffuser. The charging currents measured during this series of tests are summarized in Table I. The currents listed are those measured after combustion chamber pressure was developed--immediately following activation of the ignitor randomly varying currents of both polarities were measured. Inspection of the charging current data in Table I indicates that, in each case, the current to the diffuser and the current to the motor were of opposite sign and of comparable magnitude. Thus the net current to the motor-diffuser system was very small and the greater part of the current measured to either one of the elements was the circulating component.

Table I

MOTOR CHARGING SUMMARY

	Motor 1 2-27-63	Motor 2 4-17-63	Motor 3 6-11-63
Fuel	Basic Fuel	Aluminized	Aluminized
Motor Charging Current (μA)	10-60 pos.	160-210 pos.	> 1000 neg.
Diffuser Charging Current (μA)	6-35 neg.	> 120 neg.	> 1000 pos.

Because of the large circulating currents, the data from the two aluminized motors are believed to shed little light on rocket motor charging rates. A discussion of these results has been included, however, for three reasons. First, the data from these tests have been previously published without qualification and have often been quoted as being indicative of rocket motor charging rate.[7,8] Since these data are probably not valid motor charging data, it was felt that the experiments should be described in some detail and that the discrepancies in the data should be pointed out so that reliance on the data will be deemphasized.

The second reason for including the results of these experiments is to point out some of the pitfalls that may await those who would measure charging currents during a static firing. As these experiments indicate, extreme care must be exercised in designing the experiment to avoid problems similar to the circulating problem encountered in these experiments. In general, if the exhaust plume plays on any conducting body that is grounded (even through a fairly high resistance path), the charging current measurements may be corrupted by a circulating component of current that flows through the conductive exhaust flume, motor, and measuring instrument. As the results of the two aluminized motor firings point out, the direction, as well as the magnitude, of the charging current may be affected. For this reason, it is advisable to make charging current measurements with the motors exhausting vertically upward in an open area, so that exhaust plume cannot play on the ground, test bay walls, fences, or other conductive appurtenance.

The results of these experiments are also of interest for another reason. It has been postulated that if staging occurs while a rocket vehicle is charged to a high potential, a large difference of potential will be generated between the separating stages, either because of asymmetrical separation or because the engine actively charges the active stage while the expended stage contains no active charging mechanism. The results of these experiments with the diffuser clearly indicate that the two parts of the staging vehicle will be electrically connected through the conductive exhaust plume as long as the motor exhaust plume

plays on the expended state. It is hardly conceivable, therefore, that significant differences in potential (i.e., more than a few tens of volts) can be developed between separating sections during a staging event in which the upstage motor is ignited at or before the time of stage separation. This conclusion is further supported by the results of experiments described in the following section with the ethylene-oxygen motor.

Only three static firings of the 5-inch solid-fuel rocket motors were made in the series of tests described above, so that it was not possible to conduct additional short circuit current measurements on these motors. Arrangements were made, however, to use a small ethylene-oxygen motor to perform additional experiments in the laboratory. The ethylene-oxygen motor, which was used primarily for experiments to study the electrical properties of the exhaust flame, had the advantage that it could be fired and seeded with very little set-up time. In addition, the fuel mixture and flow rate could be varied during a run, and the motor could be burned continuously for extended periods of time.

The ethylene-oxygen motor was installed in a 4 × 4 × 8 foot metal vacuum chamber equipped with a high-speed mechanical vacuum pump capable of maintaining the pressure at 10 to 20 mmHg while the motor is burning. As in the case of the solid fuel motor experiments the motor was insulated from ground. To simulate the diffuser tube used with the solid fuel motors, a brass tube was mounted over the exhaust plume above the burner and electrically isolated from the burner with a section of glass pipe. The combustion chamber contains an igniter wire which is connected to a high voltage power source to ignite the fuel mixture in the burner. Provisions were made to measure the charging current to the motor, diffuser, and igniter individually or in any combination.

A detailed description of these experiments and the results obtained is given in Appendix A. Essentially, it was found that the circulating currents flowing between the motor, diffuser, and igniter were always larger than the net charging current to the system as a whole. Net charging currents ranging from 1 to 4 μamp were measured while the circulating currents ranged from 2 to 23 μamp. It was noted that the current in the igniter lead was always of such a direction as to suggest that the

igniter was emitting electrons. The emission of electrons from the igniter served primarily to augment the circulating current, but did not appreciably change the net charging current to the system.

Tests in which a bias voltage was applied between the motor and diffuser indicated that the diffuser was acting as a sheath-area limited Langmuir probe, because when the diffuser is negative, it appears to be collecting a saturation ion current, while at positive diffuser potentials large electron currents are collected. For this explanation of the circulating current characteristics to be valid, however, it must be assumed that the motor is not sheath area limited. This would imply that either the electron-ion density at the motor exit plane is much higher than it is in the vicinity of the diffuser, or that the motor is capable of emitting electrons when it is at negative potentials. That the former condition is satisfied is indicated by electron density data obtained from measurements made with a similar motor under similar fuel consumption rates.

Since the diffuser is capable of collecting current of either polarity with the proper bias, one is inclined to propose this process as a method for discharging rocket vehicles. Thus, for example, one would insert a probe into the exhaust plume and bias it to collect a neutralizing current to maintain zero rocket potential. This scheme does not appear to be very promising, however, in light of the observation that the circulating currents do not appreciably affect the net charging current. To further examine this scheme, the test with the biased diffuser was repeated with one microammeter measuring net charging current and the other measuring diffuser line current. It was noted that the net charging current to the system does not change direction even though the diffuser current changes from the saturation value in one direction to a very large value in the opposite direction. It seems probable, therefore, that the biased probe scheme for discharging rocket vehicles will be ineffective.

The experiments with the biased diffuser are also interesting because of the behavior of the circulating component of current in the vicinity of zero bias. A slight change in bias voltage in this region

can produce a large change in circulating current, and the direction of current flow can be reversed with a small change in bias. It is believed that this characteristic has a bearing on the results of the static firings of the aluminized motors, in which the currents flowed in opposite directions in the two test firings. Since the exhaust of the aluminized motors is probably at least as conductive as the ethylene oxygen exhaust, a change of only a fraction of a volt in bias can reverse the direction of flow. The motor-diffuser loop undoubtedly contains some bias sources as a result of thermoelectric junctions and contact potentials. This bias can be either positive or negative, depending on the circuit components used and the manner in which they are assembled. Since the motor charging apparatus was dismantled and reassembled between the two aluminized motor firings, it is suspected that the different directions of current flow observed in the two firings was caused by different bias voltages built into the motor-diffuser loop in the two experiments.

B. Motor Charging Experiments By Others

It is also of interest to compare the results of these charging current experiments with the motor charging experiments conducted by others. Although few static firings have been conducted for the purpose of investigating electrostatic effects, some interesting results have been reported. The Boeing Company has, for example, fired a number of small, solid-fuel motors in the 200-to-500-pound-thrust range to determine motor charging currents.[9] These motors were fired in a horizontal position in test bays that had metal structure aft of the exit plane and quite close to the visible portion of the plume. Charging current was measured with essentially zero potential on the motor. Charging currents of less than 0.1 μamp were measured on the 200-pound-thrust motors, but the results from these motors were not considered typical because of unsatisfactory thrust-time curves. The 350-pound-thrust motors charged at a 1 μamp rate initially (for about 0.2 sec), after which the charging rate dropped to 0-to-0.5 μamp. The 500-pound-thrust motors also charged

to 1 μamp during the first 0.2 sec, after which the charging rate varied from 0 to about 2.5 μamp. The direction of the charging current was such as to charge the motor to negative potentials.

Although the validity of those experiments is questionable because of the nearby metal structure, the charging rates seem reasonable. If circulating currents were present because of the structure, they were much smaller than the circulating currents observed in the static firings described in Section II A. It is stated in Ref. 9 that the plume (presumably the visible plume) did not touch the metal structure; hence smaller circulating currents would be expected in this case than in the case where the diffuser tube is in direct contact with the visible plume. The Boeing motors and the motors described in Section II A were of similar size, burning time, and fuel. (The Boeing motors were cast with Minuteman first stage propellant.)

Another static firing of a solid-fuel motor in which charging current was measured has been reported by workers at the Applied Physics Laboratory.[10] Unfortunately, the characteristics of the motor are not given, and the charging characteristics of the motor are presented in such a form that neither the short-circuit current nor the open-circuit potential can be determined. The polarity was not given.

The NASA Langley Research Center has performed static-firing experiments using small solid-fuel motors exhausting into a 40-foot-diameter spherical vacuum chamber maintained at a pressure of approximately 1 mmHg.[11] The propellant was polyurethane doped with aluminum. The motor potentials were measured during several tests and the charging current was measured on at least one motor. The motors charged negatively to about 10 volts during ignition and positively to 10 to 20 volts during burning. The polarity and reversal of polarity are not easily explained, but they do not appear to be unusual. It is interesting, however, that the motors charged to potentials of only a few tens of volts. This result seems to substantiate the theory that the conductivity of the exhaust plume limits the motor potential to very low potentials at high altitudes where the ion mobility is high, and

the results are in general agreement with the observations on jet engine charging (except for polarity). There is some question, however, as to the validity of these experiments because of the possibility of the exhaust plume touching the chamber walls. At pressures of the order of 1 mmHg, the physical dimensions of the exhaust plume are much greater than at sea level. Hence the plume may have reached the sides of the vacuum chamber and provided a conductive path to the grounded chamber walls. Even if this were the case, the results are interesting since they would then illustrate the effectiveness of the exhaust plume in minimizing the potential difference between the motor and adjacent structures (for example, during stage separation).

Some interesting experiments with charging were conducted by the Germans during World War II in connection with an investigation of failures of a radio-controlled glide bomb.[12] In these experiments, the torches* were burned in wind tunnels and the open-circuit potentials were measured. In one experiment, the motors were mounted on a control surface and burned in the airstream of a large propeller which generated wind velocities of 20 m/sec (45 mph). Triboelectric charging from dust picked up by the wind stream charged the control surface to about 100 volts before the motor was ignited. After ignition, the motors charged the control surface to a maximum of 325 volts. In another test the motors were placed in a wind tunnel capable of speeds up to 230 m/sec (500 mph). At the maximum wind tunnel speeds, the motors charged to as high as 6,000 volts. In the wind tunnel, however, the air recirculated once every 4 sec, so that the air flowing by the motors was free of combustion products only during the first four seconds of motor burning. The maximum potentials were observed more than 4 sec after ignition (total burning time was 1-to-2 minutes). Some concern was also expressed about the effect of a grounded metal screen 20 meters downwind from the motors in the wind

---

* Reference 12 is a translation of a captured German document originally printed in German in 1941. The translation is rather poor, however, and some of the technical terms are garbled. The word "torch" is consistently used to denote the device tested, but from the text it appears that the device was a small rocket motor.

tunnel. The maximum potential attained was found to be fairly constant at wind speeds up to 150 meters per second. At wind speeds of about 200 m/sec, however, the maximum potential increased sharply with wind speed. It is not clear whether this increase is due to increased blow-away current, to increased triboelectric charging from exhaust particles in the wind stream, or to some other mechanism. It is noted that of the two motor types, which are referred to as smoke and smokeless torches, the smokeless torches charged to lower potentials than the smoke torches. It is also noted that the motors charged positively.

C. Motor Potential Measurements

Because of inconsistencies among the motor charging data available and uncertainties concerning the various experimental set-ups, a second set of static firings was scheduled. (The results of these firings are described in detail in Appendix B.) These motors were fired for the sole purpose of measuring charging characteristics, so that it was not necessary to compromise the charging experiment to accommodate other experiments. In addition, rather than measure short circuit charging current, it was decided to measure open-circuit vehicle potential. This decision was based on experience with flames and other plasma systems that suggested that the conductivity of the highly ionized exhaust plume would tend to limit the potential to which a rocket motor could charge. It had also been observed that the maximum potential acquired by the first Nike-Cajun (see Section III) during motor burning was well below the corona threshold potential. The rather low potentials observed in the NASA and in the German experiments seemed to substantiate the potential limiting action of the ionized exhaust also.[11,12]

The motors used in these tests were similar to those used in the earlier static firings described in Section II A and in Appendix A. To eliminate the effects of conducting walls or other objects in or near the exhaust, the motors were fired in an open field with the exhaust directed vertically upward. Provisions were made to isolate the motors from ground using a structure such that, with 150 kV applied, the leakage and corona

currents were less than 1 μamp. A rotating-vane field meter was used as an infinite impedance voltmeter to measure the potential of the motor.

A total of five 5-inch polyurethane and ammonium perchlorate motors were fired in this series of experiments. Three of these contained only a 1 percent potassium seed, and the other two contained the 1 percent potassium and 15 percent aluminum. Burning time for the motors was about 3 sec.

In the initial test, one potassium seeded motor and one aluminized motor were fired from the insulated fixture. The potassium seeded motor charged to slightly over one kilovolt (positive) during the first second of burning and remained at that potential. The potential attained by the aluminized motor was only 200 volts (positive). It had been anticipated that the ionized exhaust plume would tend to limit the potential to which the motor would charge, but it was not suspected that the potential would be limited to such low values.

Although the potentials were much lower than had been anticipated, there appears to be a logical pattern in the ultimate potentials. Since the aluminized motor is characterized by a greater electron density in the combustion chamber and exhaust, the plume is more conductive and is a better discharger. Thus one would expect that the exhaust plume of the aluminized motor would limit the potential to a lower value, as was observed.

The remaining motors were used to perform experiments to test the electron diffusion theory of engine charging and study the effect of fields in the vicinity of the plume in discharging the motor. It was reasoned that if electron diffusion were the charging mechanism in jet engines, the same mechanism should operate within the combustion chamber of rocket engines. If the exhaust plume were highly conductive, however, the rate of capture of ions from the exhaust might be sufficient to essentially eliminate the effect of electron diffusion charging. However, if the exhaust were in a field-free region until the electrons attached to neutral molecules and some recombination occurred, the rate of capture of ions from the exhaust should be greatly reduced and the ability of the

plume to discharge the motor should be considerably reduced. To provide a field-free region about the plume, the plume must be surrounded with a conductive cover so that the electrostatic field lines terminate on the cover instead of the plume.

Accordingly, a tube 2 feet in diameter and 10 feet high was fabricated from 1/4-inch mesh hardware cloth and installed over the motor mount. The hardware-cloth tube prevented static fields from reaching the exhaust plume, yet allowed flow of air and exhaust gases in the exhaust region. The upper end of the tube was covered with hardware-cloth, so that the entire visible plume was within the electrostatic shield.

Two motors, one with the potassium seed and one aluminized, were fired within the closed shield described above. The potassium seeded motor initially charged positively, but in about 0.3 sec the polarity reversed, and the motor charged negatively for the remainder of the burning period, reaching a maximum negative potential of about 1.2 kilovolts. The aluminized motor charged positively for most of the burning period, reaching a maximum potential of slightly over 9 kilovolts.

Before firing the third motor in the shielded configuration, the hardware-cloth end closure at the top of the shield was removed, leaving only the cylindrical walls of the shiled. The sides of the plume were thus shielded from electrostatic fields, but because of fringing at the upper end of the shield, it may have been possible for some field lines to terminate on the end of the plume. The potassium seeded motor fired in this open-end shield configuration charged negatively throughout the burning period, but the maximum potential attained only about 260 volts.

The tests with the closed shields suggest that the discharging capability of the plume is reduced somewhat if the highly conductive part of the plume is shielded from the electrostatic fields of the charged motor. This indication is particularly strong in the case of the aluminized motors. The unshielded motor charged to only about 200 volts, while the shielded motor charged to over 9 kilovolts. The effect of shielding the plume is less striking in the cases of the nonaluminized motors, but even here, the closed shield appears to have enhanced the maximum motor

potential slightly. The shield used in these tests is not perfect, of course, because even though the exhaust has cooled and the electrons have become attached to molecules to form less mobile negative ions, the ions must pass through the screen and escape in order for charging to occur. But by the time the ions reach the screen, the gas velocity is lower, so that the probability of them being captured by the screen is enhanced. In addition, the wind velocity induced outside the screen is much lower than the wind velocity induced in the absence of the screen, so that the chance of the ions being blown away is less.

It is suspected that there are also other shortcomings of the static firing experiments that limit the degree to which actual rocket motors in flight are simulated. In the tests reported here and in most of the tests reported in the literature, the burning time of the motors was only about 5 sec, whereas burning time for most launch vehicles is an order of magnitude greater. The effect of the thermal conditions and ablation in the nozzle for motors that burn longer than 5 sec is not known. Another point of dissimilarity is the ambient pressure which, while constant at sea level pressure in static firings, varies from the sea level value to many orders of magnitude less than sea level on launch vehicles. Finally, the air flow about the motor in static firings is quite different from the flow about flight vehicles. In the static firings, the only air flow existing is that induced by the exhaust gas flow, and in the region of the nozzles where outside air flow is most influential, flow patterns are distorted by the structure supporting the motor. In flight vehicles, however, relatively unobstructed air flow is produced by the forward motion of the rocket, as well as the motor exhaust. In spite of these shortcomings which limit the significance of the absolute potentials and charging currents measured, the static firings do provide an economical method of studying charging mechanisms, and further effort in this direction should be productive.

III NIKE-CAJUN EXPERIMENTS

A. First Nike-Cajun Experiment

Although static firing experiments of the type described in Section II are informative and convenient to conduct, data from flight vehicles are essential to provide a basis for evaluating the validity of laboratory simulations. An effort was therefore made to obtain data on vehicle potentials from instrumentation installed on Nike-Cajun vehicles when space and weight were available. In these experiments, instrumentation was limited to a single rotating vane field meter installed to measure the electric field strength at the surface of the vehicle. From measurements made in the laboratory on scale models of the vehicle, the vehicle capacitance and the relation between the vehicle potential and the field strength at the field meter location were determined. It is thus possible to calibrate the field meter response in terms of vehicle potential, and from the rate of change of vehicle potential and the capacitance, the charging rates and discharging rates can be estimated.

The first flight of an instrumented Nike-Cajun occurred 14 March 1961 from Eglin Gulf Test Range.[13] Because the field meter was designed and fabricated within a few weeks (upon learning what space and weight would be available on the Cajun), phase and polarity discrimination were not incorporated into the field meter system. Polarity of the vehicle potential was not determined, therefore, and in the ionosphere, the field meter could not distinguish between a convection current (electron or ion collection by the field meter stator) and a true electric field. The field meter was located on the cylindrical body of the Cajun vehicle a few inches aft of the nose cone as illustrated in Fig. 2. Two field meter sensitivities, 0-to-50 kV/m and 0-to-500 kV/m were provided. The field meter appeared to function properly, within the limitations indicated, throughout the flight. The indicated field strength for the

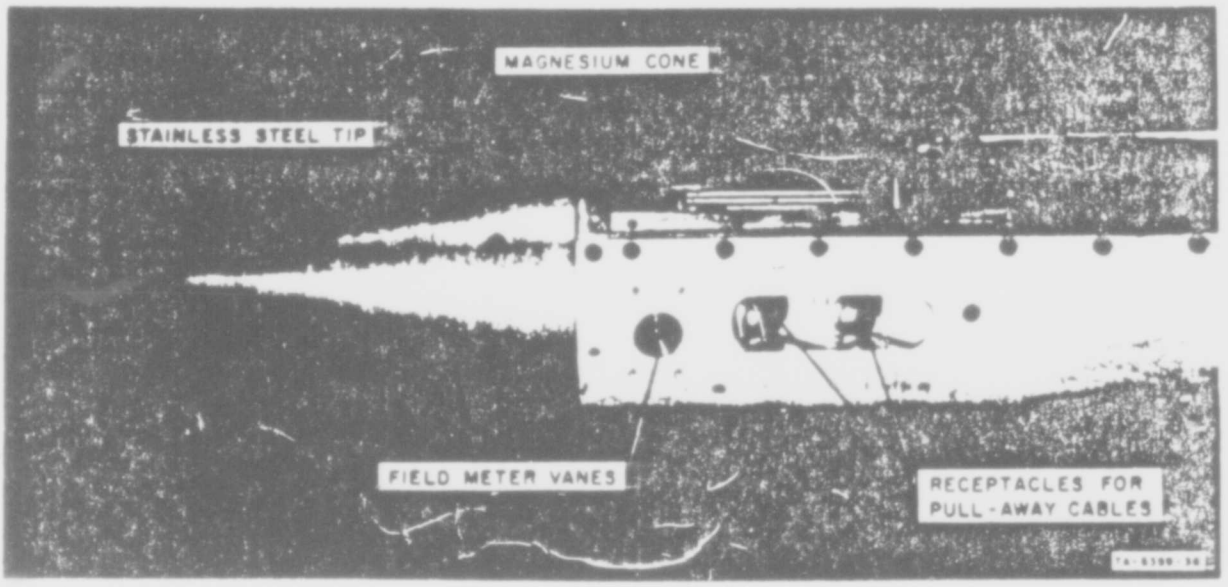

FIG. 2 NIKE-CAJUN PAYLOAD SHOWING FIELD METER LOCATION

entire flight is shown in Fig. 3 in terms of field strength at the field meter. The field strength at the field meter is related to the vehicle potential by

$$E = 3.6\ V$$

where E is the field strength in kilovolts per meter and V is the potential in kilovolts.

The effect of the Nike motor and the Cajun motor on the vehicle potential is apparent in Fig. 3. From the relation between field strength and vehicle potential, the maximum potential during Nike burning is observed to be about 26 kilovolts. This potential is well below the threshold potential of 170 kilovolts for corona discharges from the Nike-Cajun tail fins at sea level. During Cajun burning, the maximum vehicle potential was only about 2 kilovolts at 12 kilometers, compared to a corona threshold potential of 35 kilovolts for the Cajun vehicle at 12 kilometers. In both cases, therefore, the maximum potential produced by the engines was about an order of magnitude lower than the vehicle corona threshold potential. (Corona threshold potentials were determined by electrostatic modeling techniques described in Reference 1.)

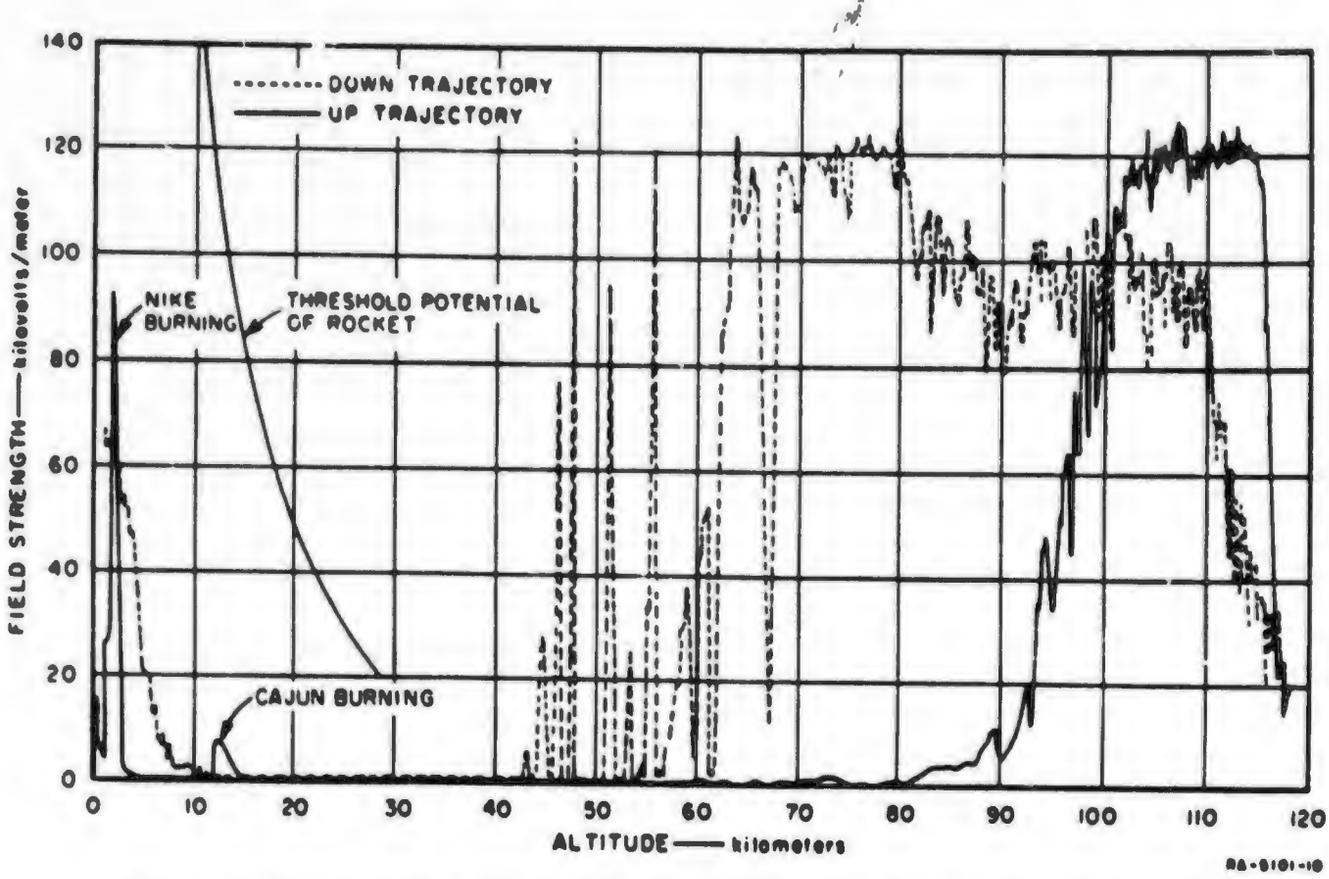

FIG. 3 ELECTRIC FIELD STRENGTH AS A FUNCTION OF ALTITUDE ON FIRST NIKE-CAJUN ROCKET

During ascent, the vehicle potential decayed to zero shortly after the Cajun burnout (burning time for the Nike and Cajun motors is about 3 sec each). At about 80 kilometers, the field meter began indicating an apparent field strength that increased to a maximum of 120 kilovolts per meter between 100 and 115 kilometers. On descent, the field meter also indicated high apparent field strengths down to 60 kilometers, and intermittently down to 42 kilometers. Below 42 kilometers, the indicated field strength was zero until the vehicle was below 10 kilometers, where very light precipitation charging apparently was encountered.

The behavior of the field meter response above 60 kilometers was initially very puzzling, because it had been anticipated that the conductivity of the ionosphere would be sufficient to maintain the vehicle potential at a very low value above 60 kilometers, and it was not readily apparent that a mechanism for producing a current flux of sufficient density to cause the observed field meter response was available.

Careful examination of the field meter circuit also failed to reveal a failure mechanism that would lead to the observed response. In fact, it was not until after a second Nike-Cajun was launched with a more refined field meter system that the cause of the behavior at high altitudes became evident. This anomaly is now believed to be associated with the antenna breakdown experiments that constituted the primary experiments on both flights. A more detailed description of the phenomenon will be given in the discussion of the second Nike-Cajun experiments; however, the conclusion reached is that above 80 kilometers during ascent and above 40 kilometers during descent, the field meter responded to a current flux rather than a true electric field, and that the vehicle potential was probably near zero throughout this altitude range.

B. Second Nike-Cajun Experiment

Because the first Nike-Cajun experiment indicated an unexplained electrical activity at altitudes above 60 kilometers (in the ionosphere), a second Nike-Cajun experiment was prepared. Special care was exercised in designing the field meter system for this experiment to discriminate between true field and convection current. The alternating component of the stator short circuit current in response to a convection current is nominally

$$I_c = \frac{1}{2} JA \qquad (1)$$

where J is the current density flowing toward the stator (when the stator is uncovered) and A is the surface area of the stator. The alternating component of the stator short circuit current in response to a true field is

$$I_f = \frac{1}{2} j\omega\epsilon_o EA \qquad (2)$$

where ω is the radian frequency with which the stator is covered and uncovered, ϵ_o is the permittivity of free space, E is the field strength of the electric field terminating on the stator (when the stator is uncovered), and j is the imaginary unit $\sqrt{-1}$. Since the response to convection currents is 90 degrees out of phase with the response to

electric field, a coherent detector using a stable reference signal synchronized with rate at which the rotor covers and uncovers the stator can be used to discriminate between the field response and the current response of the stator. In the field meter system used on the second Nike-Cajun experiment, the reference signal was obtained from a reference generator driven by the motor used to drive the field meter rotor. Since the stator signal frequency and the reference generator frequency are both determined by the mechanical speed of the drive motor, the phase difference between the stator signal and the reference signal is independent of the drive motor speed. To prevent excessive variation of motor speed during periods of high acceleration and wind loading, however, a speed control circuit was incorporated into the motor power supply.

Similar field meter systems using coherent detectors have often been used in airborne and ground field measurements because the coherent detector permits one to determine polarity of the field as well as field strength. In these systems, however, only the "in phase" component of the stator signal is normally detected. That is, the response to the electric field is detected and the response to convection currents, which is usually negligible at altitudes below 60 kilometers, is rejected. By using a second coherent detector adjusted to respond to stator signals in phase-quadrature with the field-produced signals, the response of the field meter to convection currents as well as electric fields can be obtained. Although this quadrature response of the field-meter is not a very useful physical parameter, it does provide a basis for evaluating the behavior of the field meter in the ionosphere. In the field meter developed for the second Nike-Cajun experiment, therefore, both the "in phase" and "quadrature" components of the stator signal were detected. Separate reference signals were generated for each coherent detector by variable reluctance pickups driven by the rotor drive motor and mechanically adjusted for the proper reference signal phase. On this vehicle, the field meter was also packaged in a separate section aft of the main Cajun payload as illustrated in Fig. 4. The field meter package containing the sensor, electronics, and

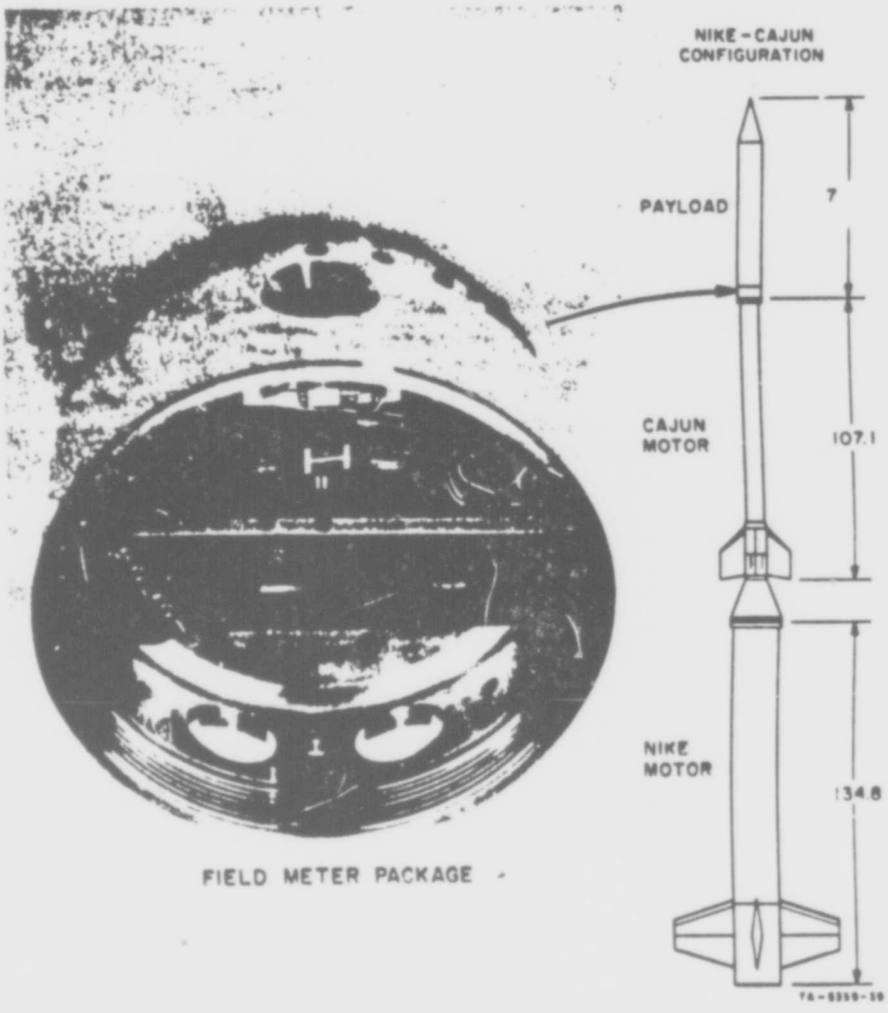

FIG. 4 FIELD-METER PACKAGE FOR SECOND NIKE-CAJUN EXPERIMENT

batteries is also shown in Fig. 4. The reference generators can be seen directly in board from the field meter vanes in Fig. 4. Two field strength sensitivities, 0-to-50 kV/m and 0-to-500 kV/m and corresponding sensitivities in response to convection current were recorded. For the field meter location used in this experiment the field strength E in kV/m is related to the vehicle potential V in kV by E = 2.4 V.

A block diagram of the field meter system is shown in Fig. 5. As illustrated, the stator signal is amplified by two separate amplifier stages to provide the two sensitivities, and the amplified signal is supplied to the coherent detectors. The "in phase" reference signal from the variable reluctance reference generator is amplified, shaped, and supplied to each of the "in phase" detectors. The quadrature system is identical to the "in phase" system except for the phase of the

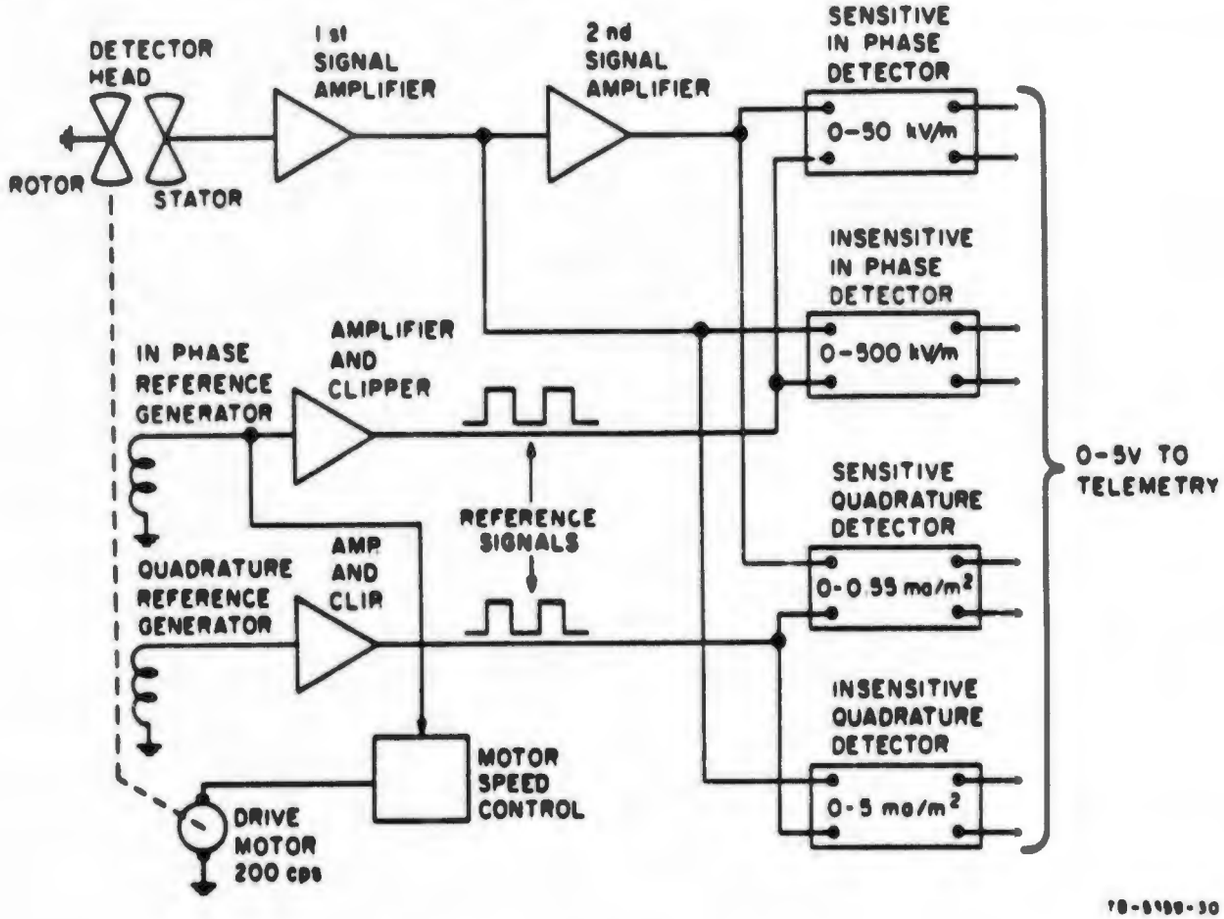

FIG. 5 BLOCK DIAGRAM OF FIELD METER SYSTEM

quadrature reference signal. The phase of the reference generator signals is adjusted by adjusting the mechanical position of the pickup coils about the iron reference generator rotor (see Fig. 4). Prior to flight, the reference generator phases were very carefully adjusted to provide maximum discrimination between true fields and convection currents. The frequency of the "in phase" reference generator signal was also used as a motor speed reference in the drive motor speed control.

The second Nike-Cajun equipped with the field meter experiment was launched 20 April 1965 at 17:04 EST from Wallops Island and reached an apogee of 341,000 ft. The field meter system appeared to function properly throughout the flight. The vehicle potential deduced from the field meter response at altitudes below 25 kilometers is shown in Fig. 6 for both the ascent and descent. The vehicle potential during Nike burning appears to be quite different from the potential for this period

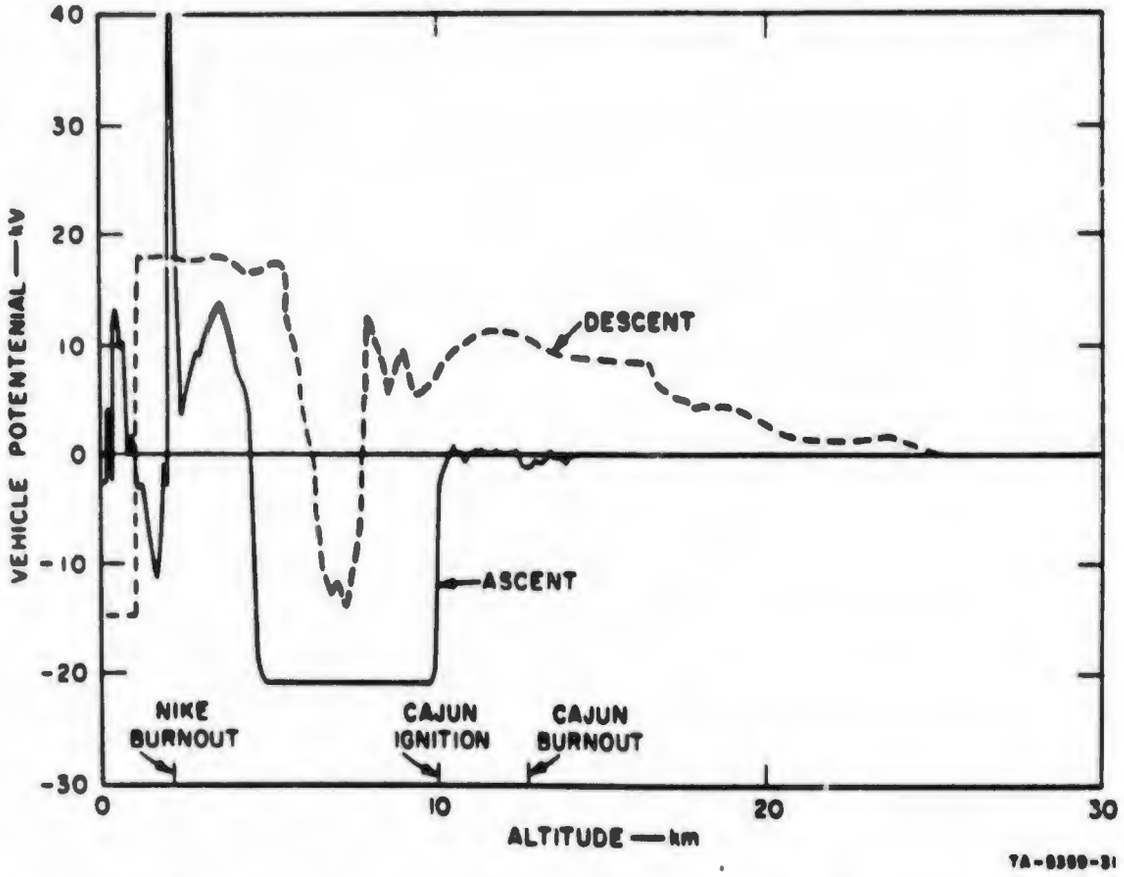

FIG. 6 VEHICLE POTENTIAL AS A FUNCTION OF ALTITUDE ON SECOND NIKE-CAJUN

on the first Nike-Cajun (see Fig. 3). Part of this difference is undoubtedly due to the fact that polarity as well as magnitude are shown in Fig. 6, while only magnitude is shown in Fig. 3. It is noted that the second rocket charged positively after some initial transients, then reversed polarity and charged negatively, then just before burnout of the Nike motor reversed polarity a second time to attain a maximum (positive) potential of 40 kilovolts.

In the separation and coast period between Nike burnout and Cajun ignition the vehicle potential remained positive until at about 4.5 kilometers, where the potential changed over a small range in altitude from +15 kilovolts to -20 kilovolts. The potential remained at a negative potential (about 20 kilovolts) for the rest of the coast period. This behavior during the coast period is quite different from the behavior of the first Nike-Cajun which remained at zero potential throughout the coast period. Although the exact cause of the vehicle potentials during this period are unknown, it is thought that the potential during this period may have been influenced by the presence of precipitation particles and, possibly, the manner in which burnout of the Nike motor occurred. As is indicated in Appendix B, during static firings some motors remained charged after burnout while others were discharged during burnout, apparently by post-burnout combustion. The first Nike-Cajun was, possibly, discharged by this post-burnout combustion, while the second rocket remained charged. If no additional charging had occurred, however, the vehicle potential would have remained constant (or decayed slightly) until Cajun ignition. It appears, therefore, that the second vehicle must also have encountered some light triboelectric charging from atmospheric dust and precipitation during the coast period. Between Nike burnout and the polarity reversal at 4.5 kilometers, the positive fluctuation in potential could have been produced by triboelectric charging from atmospheric dust. Pollens and dusts of clay and ores have been observed to produce positive charging of metal bodies in related experiments.[8] The polarity reversal at 4.7 kilometers may have been caused by a thin layer of cirrus particles (ice crystals normally charge vehicles to negative potentials). Above 5 kilometers the

potential does not change significantly until Cajun ignition. This would indicate that significant charging activity ceased at 5 kilometers and the charge the vehicle had at this altitude remained on the vehicle until Cajun ignition. It should be noted that the triboelectric charging rates required are extremely low, since at no time did the vehicle potential approach its corona threshold value. At these altitudes the only effective loss mechanism other than corona is air conductivity, which is very low.

At Cajun ignition the -20 kilovolt potential that the vehicle had during the latter portion of the coast period was quickly discharged to zero. This behavior also differs from the observed behavior of the first rocket in which the vehicle was charged to 2 kilovolts during Cajun burning, but this probably results from minor differences in the motors (during static firings, for example, potentials varied from a few hundred volts to a few kilovolts from one motor to the next). In addition, it was not possible to accurately measure potentials less than 1 kilovolt on the second rocket because of the noise level (or commutator jitter) and the scale compression necessary to accommodate both positive and negative potentials. In neither case did the Cajun motor, burning at altitudes greater than 10 kilometers, produce charging that would be of any consequence on a properly bonded vehicle. The results from the second rocket are interesting because they demonstrate that a charged vehicle can be discharged by the rocket exhaust at high altitudes.

After the vehicle had been discharged by the Cajun motor, there was no further indication of charging activity until the vehicle reached an altitude of about 25 kilometers on descent. Below 25 kilometers the vehicle potential varied somewhat randomly, reaching a maximum negative potential of 14 kilovolts at 7.4 kilometers and a maximum positive potential of 18 kilovolts at 1.0 kilometers. A similar acquisition of potential was observed below 10 kilometers during the flight of the first rocket (see Fig. 3). The cause of these potentials is not known, but it is suspected that they may also be attributed to dust and precipitation in the lower atmosphere. As in the case of the potentials observed

during the coast period on the second rocket, the charging rates are extremely low, since the potentials do not approach the corona threshold potential of the vehicle.

Although there was no indication of vehicle potentials capable of being detected by the field meter at altitudes above 25 kilometers, the field meter did respond to convection currents produced by other experiments in the payload. On both Nike-Cajun flights, the primary payloads were antenna breakdown experiments designed to determine the power levels required to produce electrical breakdown of VHF and X-band antennas as a function of altitude. For these experiments a VHF quadrapole antenna and an X-band slot antenna were mounted on the vehicle and supplied with periodically varying RF power. The period of the breakdown power cycle was 1 sec, during which the RF power was increased from zero to its maximum value and reduced to zero again. As the vehicle reached altitudes where the ambient pressure was low enough that the peak RF power was capable of producing breakdown at the antenna, a plasma was periodically produced about the antenna.

Jackson and Kane have pointed out that a rocket-borne antenna such as an electric dipole will capture electrons from a neutral plasma such as the ionosphere.[14] When the electron mean free path is short, compared to the free space amplitude of oscillation of the electron, the antenna and rocket form an asymmetric Langmuir probe in which the current is limited by the sheath area of the antenna. Since the electron current collected when the antenna is positive is much greater than the positive ion current collected when the antenna is negative, a net electron current is collected until the vehicle becomes slightly more negative than the normal equilibrium potential. As the vehicle becomes more negatively charged, however, the positive ion current to the surface of the vehicle is increased. The net positive ion current to the vehicle is equal to the net electron current collected by the antenna at equilibrium.

In the normal ionosphere the electron density is so low that the currents produced in this manner are quite small. For an electron

density of 10^5 cm^{-3}, an electron temperature of 200°K, an antenna sheath area of 100 cm^2, and an antenna voltage greater than a few volts, the electron current collected by the antenna will be only about 2 μamp.[3] The neutralizing ion current of 2 μamp is distributed over the entire surface of the vehicle, so that the current density on the vehicle surface is very small. When antenna breakdown occurs, however, a much more dense plasma is produced about the antenna. From this dense plasma the antenna can collect a relatively large electron current; for example, with electron densities of the order of 10^9 cm^{-3} produced by VHF discharges, the electron current to the antenna could be of the order of 50 mamp.

At lower pressures, where the electron mean-free-path is large compared to the amplitude of oscillation of the electron in the RF field, the nonuniform electric field about the antenna can cause electrons in the plasma to "walk" away from the antenna. This phenomenon can be demonstrated by considering the behavior of an electron placed in the nonuniform field of a short cylindrical antenna. If the electron is released near the surface of the antenna at the instant that the negative half-cycle of the antenna field begins, the electron is accelerated away from the antenna by the strong fields near the antenna. The further from the antenna the electron moves, the weaker the field (per unit of antenna voltage) becomes because of the nonuniformity of the field. Thus when the succeeding positive half-cycle begins, the field accelerating the electron back toward the antenna is much weaker, and the displacement of the electron toward the antenna during the positive half-cycle is less than the displacement of the electron away from the antenna during the negative half-cycle. As a result at the end of each succeeding RF cycle, the electron is a little further from the antenna than it was at the beginning of the cycle.. Similar action occurs with positive ions, but because of the much greater mass of the ions, the ion drift rate is much less than the electron drift rate.

Under conditions of high frequency and large mean free path, an asymmetric antenna tends to repel electrons, and if a copious supply of electrons is generated in the vicinity of the antenna, a flux of electrons will flow away from the antenna. The electrons can be supplied

by a secondary-emission controlled (multipactor) discharge or a discharge in which secondary emission is an important contributor of electrons. Under very high field conditions, the electrons may also be produced by collision processes within the gas and by secondary emission resulting from positive ions striking the antenna. Aside from the direction of current flow, however, the effect on the vehicle is similar to that observed at higher pressures during antenna breakdown.

During the second Nike-Cajun experiment, the VHF breakdown data indicate that antenna breakdown commenced during ascent at 18.3 kilometers. At this altitude the pressure is still high enough (40 mmHg) that the discharge is attachment controlled, and the region of ionization is limited to the immediate vicinity of antenna. In addition, the vehicle is well below the ionosphere, so that the only current flux to the body of the vehicle would be the current drawn from the discharge products. The field meter did not respond to the VHF antenna breakdown at this altitude.

At 61 kilometers, the field meter's sensitive quadrature detector began to respond to the VHF antenna breakdown. At this altitude the pressure is about 0.2 mmHg--approximately the pressure for minimum antenna breakdown voltage. It is also the approximate altitude of the bottom of the ionospheric D-layer. Thus at this altitude two phenomena may contribute to an enhanced current flux to the body of the rocket; the presence of ambient ionization from the ionosphere, and the growing region of ionization produced by the antenna breakdown as electron attachment becomes a weaker loss mechanism.

Figure 7 shows the decommutated telemetry record of the sensitive channels of the field meter and the incident RF power to the VHF antenna in the region where the quadrature (convection current) response of the field meter became noticeable. The period of antenna breakdown is clearly recognizable in the incident power record by the sudden drop when the breakdown initiates and the slight increase when the discharge extinguishes. It is noted that the quadrature response of the field meter is coincident with the period of antenna breakdown. (The field meter data

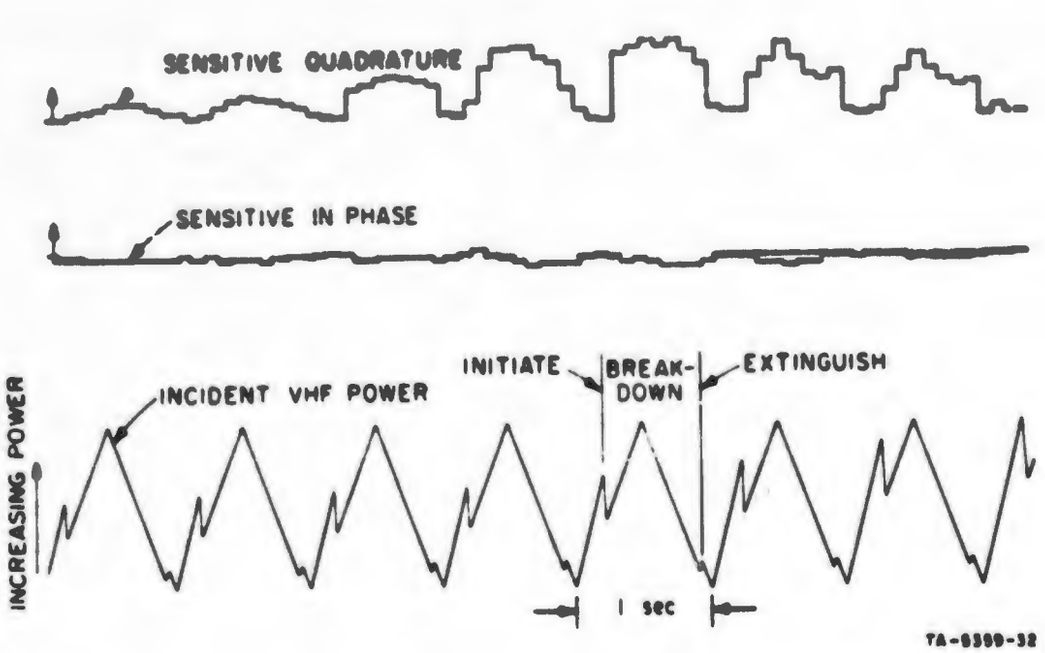

FIG. 7 IN-PHASE (field) AND QUADRATURE (current) RESPONSE OF FIELD METER DURING VHF ANTENNA BREAKDOWN BETWEEN 61 AND 67 KILOMETERS. (Reproduced from decommutated telemetry data.)

were sampled at the rate of 10 samples per second, thus giving a stepped appearance to the field meter data.)

As the rocket altitude increased, the response of the field meter to the antenna breakdown increased until at 73 kilometers, the amplifiers driving the sensitive quadrature detector saturated. Prior to saturation of the sensitive quadrature detector, the "in phase" response of the field meter was zero, but upon amplifier saturation the sensitive "in phase" detector also began indicating an output because the same saturated amplifier supplied the signal to the sensitive "in phase" detector (see Fig. 5). The output of the sensitive "in phase" detector was thus the result of a distorted signal from the saturated amplifier rather than an indication of a detectable electric field. After saturation of the sensitive quadrature detector, the insensitive quadrature detector was still operating in its linear region and the insensitive "in phase" detector still indicated zero.

The field meter response in the vicinity of 73 kilometers is shown in Fig. 8, where all four field meter channels and the incident VHF power are shown. The arrows on the field meter traces indicate the direction of positive deflection for the traces, positive deflection implying positive ion collection on the quadrature channels and positive charge on the vehicle on the "in phase" channels. The coincidence of quadrature response and antenna breakdown is again obvious. The noisy appearance of the sensitive "in phase" trace is caused by the saturated amplifier supplying the sensitive detectors. Note that without a carefully phased coherent detector the quadrature response shown in Figs. 7 and 8 could mistakenly be interpreted as a true electric field.

The peak quadrature response of the field meter for the antenna breakdown periods during which a nonzero response was observed is shown in Fig. 9. The field meter response is shown in terms of a theoretical electron current density to the stator based on Eqs. (1) and (2) and the known response of the field meter to electric fields. Although the actual quadrature response of the field meter depends on a number of factors such as electron density, electron temperature, electron mean free path, and spacing between rotor and stator, preliminary experiments with the field meter in a low pressure plasma environment indicated that the actual response was of the same order of magnitude as the theoretical response.

As illustrated in Fig. 9, the field meter collected positive ions during antenna breakdown at altitudes below 90 kilometers, implying that the antenna collected electrons in accordance with the Jackson and Kane experience.[14] In the vicinity of 95 kilometers, however, the field meter collected electrons during antenna breakdown. This suggests that at 95 kilometers the antenna breakdown process produced electrons and repelled them. This breakdown period lasted only about 6 sec and was not encountered on descent. At this altitude, however, the electron mean free path is of the order of the antenna dimensions, and considerably larger than the amplitude of oscillation of an electron in moderate VHF fields. Thus if a breakdown such as a multipactor discharge occurred,

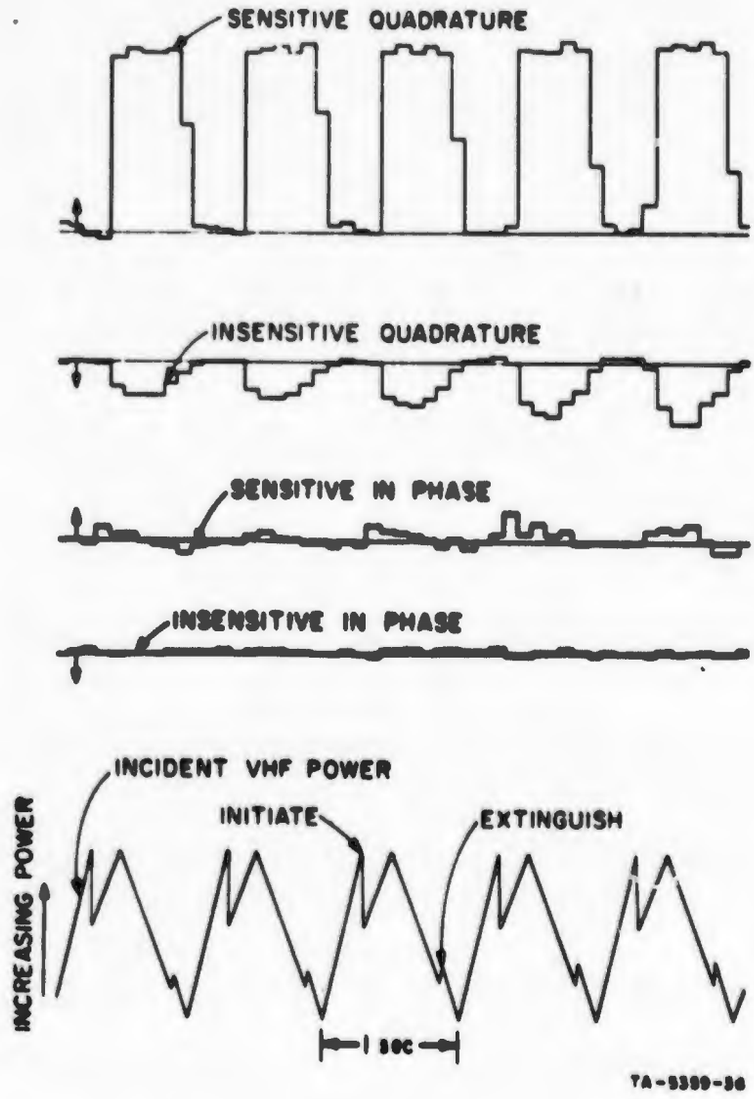

FIG. 8 IN-PHASE (field) AND QUADRATURE (current) RESPONSE OF FIELD METER ABOVE 73 KILOMETERS WHERE SENSITIVE QUADRATURE CHANNEL SATURATES. (Reproduced from decommutated telemetry data.)

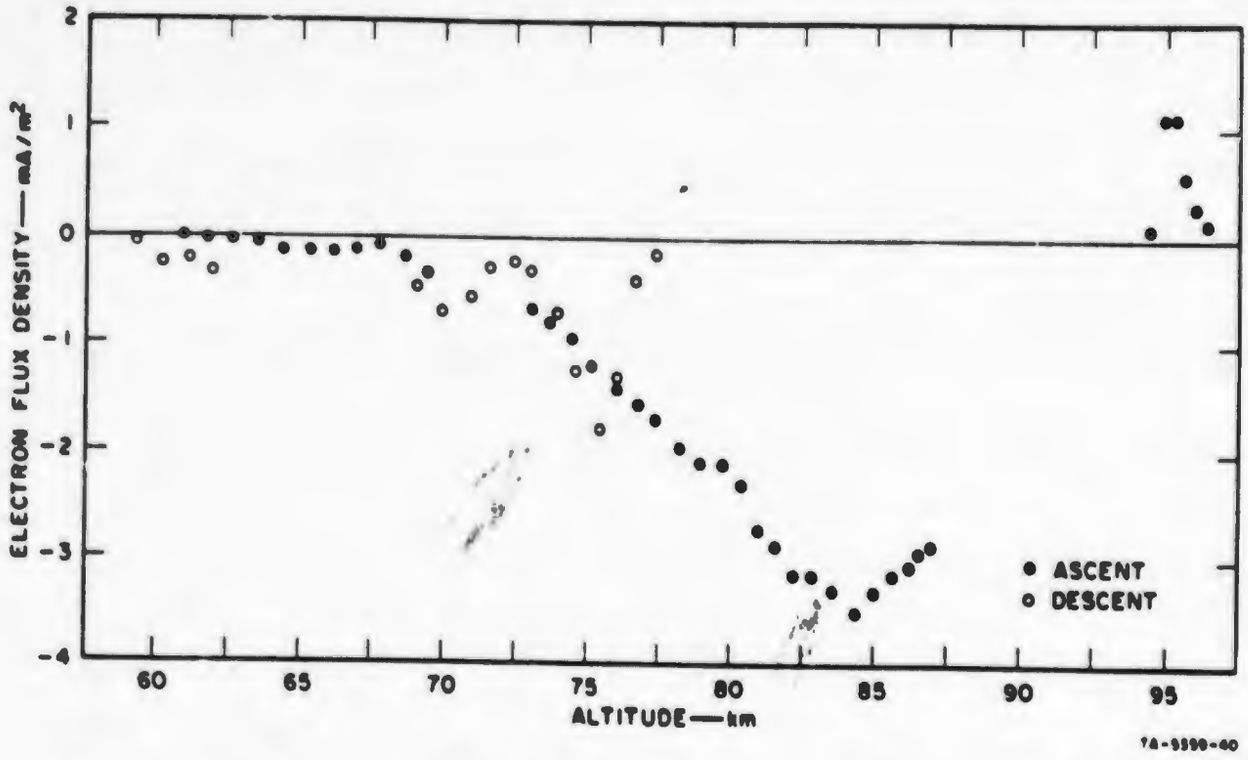

FIG. 9 ELECTRON FLUX DENSITY ABOVE 70 KILOMETERS FROM FIELD METER QUADRATURE RESPONSE. Positive flux density represents electrons captured by field meter stator; negative flux density represents positive ions captured by field meter stator.

one would anticipate that electrons would be repelled by the antenna and collected on the rocket body.

It is of interest to examine the error that would have been incurred if the current response indicated in Fig. 9 had erroneously been interpreted as the response to a true electric field. The right-hand column of Table II gives the values of vehicle potential that would be required to produce an "in phase" field meter response equivalent to the quadrature response observed during antenna breakdown. Although the actual vehicle potential was too low to be detected at those altitudes, the maximum value that it could have been without detection is indicated in the center column of Table II. It is important to note that the apparent vehicle potentials that would have been deduced from a field meter not having a good coherent detector are at least an order of magnitude too high (they are probably much worse than an order of magnitude too high, since it is difficult to conceive of the antenna

Table II

COMPARISON OF APPARENT VEHICLE POTENTIAL DEDUCED FROM CURRENT RESPONSE OF FIELD METER WITH TRUE VEHICLE POTENTIAL

Altitude (km)	True Vehicle Potential (kV)	Apparent Vehicle Potential (kV)
60	<1	4
65	<1	8
70	<1	19
75	<10	49
80	<10	84
85	<10	129

charging the vehicle to more than a few tens of volts). It is also of interest to note that the apparent vehicle potentials shown in Table II are compatible with the apparent field strengths measured on the first Nike-Cajun vehicle (see Fig. 3) in this altitude range with a field meter incapable of distinguishing between field and convection current. The apparent field strengths on the first rocket indicate apparent vehicle potentials that are continuous and somewhat lower than those indicated in Table II, but there are some significant differences in the experiments that may account for this discrepancy. On the second rocket, the antenna breakdown experiment functioned properly throughout the flight, while on the first rocket the VHF antenna breakdown experiment displayed peculiar and unexplained behavior above 20,000 ft. It is suspected that this difference in the behavior of the VHF antenna breakdown experiment is responsible for the fact that the response of the field meter on the first rocket was continuous above 60 kilometers, whereas the quadrature response of the field meter on the second rocket was observed only during antenna breakdown periods.

In addition, on the first rocket the field meter was forward of the antenna breakdown experiments (see Fig. 2), while on the second rocket the field meter was aft of the breakdown experiments (see Fig. 4).

This difference in position of the field meters may account for the fact that the current response of the field meter on the second rocket was somewhat greater than that observed on the first rocket. Because the field meter on the second rocket was downwind from the VHF antenna (although displaced about 100 degrees azimuthally), discharge products from the antenna may have reached the region of the field meter and provided an enhanced ion density over the field meter. From the quadrature response of the field meter shown in Fig. 9 and the maximum true vehicle potentials shown in Table II, it is possible to estimate the minimum positive ion conductivity σ in the vicinity of the field meter, since

$$J \leq \sigma E = 2.4\, \sigma V \qquad (3)$$

where J is the current density obtained from Fig. 9 and V is the maximum potential that the vehicle could have had without being detected on the "in phase" channels of the field meter as indicated in Table II. The minimum values of the conductivity σ deduced from Eq. (3) are shown in Table III along with the accepted values of positive ion conductivity due to ambient ion density in the ionosphere.[18] As is obvious from the table, the minimum conductivity deduced from the field meter response is 1-to-2 orders of magnitude greater than the conductivity due to ambient ionization. Since the conductivity is directly proportional to the ion density, it appears that the discharge products from the antenna enhanced the ion density at the field meter.

C. Other Flight Tests

The only other reported instrumented flight test known to the authors that is comparable to the Nike-Cajun experiments reported here is the flight of a Viking 5 rocket reported in Ref. 15 and by Whipple.[16] The Viking 5 was a one-stage liquid-fuel rocket using liquid oxygen and ethyl alcohol for the primary propellants. The primary experiments on the Viking 5 were ionosphere and polar radiation measurements; however, one of the instruments carried was a rotating vane electric field meter similar to the one used on the Nike-Cajun experiments. The rocket was

Table III

COMPARISON OF POSITIVE ION CONDUCTIVITY
INDICATED BY FIELD METER WITH ACCEPTED VALUES

Altitude (km)	Positive Ion Conductivity	
	Minimum Indicated (mho/m x 10^8)	Accepted Value (mho/m x 10^8)
60	4	0.04
65	8	0.08
70	21	0.1
75	5	0.2
80	9	0.5
85	14	1.0

launched at 1018 MST from White Sands Proving Ground, New Mexico, 21 November 1950, and reached an altitude of 175 kilometers.

During launch the maximum field strength measured on the vehicle was about 15 kV/m. Two polarity reversals were observed during the first ten seconds of flight, and the vehicle potential gradually decreased as the vehicle gained altitude.[18] In the 35 to 80 kilometer altitude range, the vehicle potential was deduced to be less than 55 volts.[18] From the relation between field strength at the field meter location and vehicle potential, the vehicle potential corresponding to the maximum field strength is about 17 kilovolts, if it is assumed that the vehicle and its plume were far enough above the launch facility that the vehicle could be considered to be in free space.

Although the Viking and Nike-Cajun motors are quite different, the charging characteristics appear to have much in common. Both vehicles charged to potentials well below the corona threshold potential, suggesting that the vehicle potential was limited by exhaust conductivity rather than corona loss. On both vehicles the limiting potential decreased with increasing altitude; and on both vehicles the potentials at ionospheric altitudes were very low (less than 1,000 volts). Both the Nike-Cajuns and the Viking were launched on clear days, so that serious

precipitation charging were not encountered. The Nike-Cajun data indicate that some extremely light charging from dust and precipitation was encountered below 20 kilometers. In this altitude range, however, the Viking motor was burning, so that light precipitation or dust charging could not be detected.

Although it appears that the charging characteristics of the slow-burning, liquid-fuel Viking rocket are quite similar to those of the fast-burning, solid-fuel Nike-Cajun rockets, the samples available at this time are too small to justify firm conclusions regarding motor charging characteristics. In addition, neither the Viking nor the Nike-Cajun very closely simulates the launch vehicles currently used for satellite and spacecraft missions, but it is doubtful that the charging characteristics of the larger vehicles are radically different from those observed on the smaller rockets. Both the Viking and the Nike-Cajun motors burn out before the vehicles reach the ionosphere, so that data on engine charging in the ionosphere are not available. Their behavior below the ionosphere suggests that engine charging will be trivial at these altitudes; however, this should be confirmed by instrumented flights. Finally, caution should be exercised in applying data from the small sounding rockets to some of the larger rockets that are covered with an insulating ablative coating and use dielectric nozzles. The potential limiting action of the plume is believed to be due to the ability of the outer surfaces of the vehicle, particularly in the vicinity of the nozzle, to collect a neutralizing current from the ionized exhaust. Additional experimental data from this type of rocket are required.

BLANK PAGE

IV REVIEW OF MOTOR CHARGING THEORY

A. Charging Current

As has been indicated elsewhere in this report, the electron diffusion theory was originally proposed to explain qualitatively the charging produced by aircraft jet engines. This theory has been further developed by Aronowitz and quantitative charging rates have been computed.[17,18] Short circuit charging rates computed by Aronowitz were in general agreement with the values reported in Section II for the static firing of the first aluminized motor. Although it is now believed that these experimental data were in error because of large circulating currents, it is apparent that the electron diffusion mechanism can produce currents of the same order of magnitude as those observed experimentally. Subsequent experimental data indicated that engine charging is positive about as often as it is negative, however. Although the electron diffusion theory for negative charging is not invalidated, some other mechanism must be postulated to account for the positive charging.

Several other mechanisms have been proposed to explain positive charging. These include photoemission from the walls of the combustion chamber and nozzle, thermonic emission from the combustion chamber and nozzle, triboelectric charging from solid particles in the combustion products striking the walls, and fuel flow and atomization (liquid-fuel motors). In addition, contact ionization, triboelectric charging, and fuel flow have been proposed as additional negative charging mechanisms. All of these mechanisms stipulate that a charged particle created in the combustion chamber or nozzle remains charged until it is effectively removed from the influence of the vehicle. As has been pointed out by Aronowitz and others, however, the hot gases in the combustion chamber and exhaust are quite conductive. Any charge created in these ionized gases is therefore quickly neutralized. Consider, for example, a rocket motor in which the following typical conditions exist:

Temperature	-	3000°K
Pressure	-	30 atmos.
Electron-ion density	-	10^{12} cm^{-3}
Exhaust velocity	-	2000 m/sec
Atomic mass number	-	28

The electronic conductivity σ_e of the combustion products is

$$\sigma_e = \frac{ne^2}{m\nu_e} \tag{4}$$

where n is the electron density, e and m are the electron charge and mass, and ν_e is the electron-neutral collision frequency. Similarly, the ionic conductivity σ_i is

$$\sigma_i = \frac{ne^2}{M\nu_i} \tag{5}$$

where M is the ion mass and ν_i is the ion-neutral collision frequency. It is assumed that the electron density is equal to the ion density (neutral plasma) and that the ions are singly ionized. Using the typical conditions above,

$$\sigma_e \approx 8 \times 10^{-4} \text{ mho/m}$$

and

$$\sigma_i \approx 9 \times 10^{-7} \text{ mho-m} \quad .$$

Since the time constant for the exponential decay of charge placed in a conductive medium is

$$T = \epsilon/\sigma \text{ sec} \quad , \tag{6}$$

the expected life of a charged particle in combustion gases is of the order of

$$T_- \quad \epsilon/\sigma_e \sim 8.85 \times 10^{-12}/8 \times 10^{-4} \lesssim 10^{-8} \text{ sec}$$

for negatively charged particles, and

$$T_+ \sim \epsilon/\sigma_+ \sim 8.85 \times 10^{-12}/9 \times 10^{-7} \lesssim 10^{-5} \text{ sec}$$

for positively charged particles. It is assumed that the negative particle is neutralized by forcing electrons to the walls of the chamber, and that the positive particle is neutralized by forcing positive ions to the walls; thus, electronic conductivity applies to negative particles and ionic conductivity applies to positive particles. In either case, however, the charged particle is effectively neutralized within a few microseconds after it is released in the combustion gases. Since the exhaust velocity is only a few millimeters per microsecond, it appears that even a positively charged particle will be discharged by the conductivity of the gases before it has traveled more than a few centimeters.

On the basis of this analysis, it would appear that any mechanism which postulates a free charge being injected into the combustion gases and carried out by the exhaust is invalid. All of the mechanisms that have been proposed would, therefore, be invalidated, except the electron diffusion mechanism which relies on expulsion of part of the positive ion sheath formed at the walls of the nozzle. But the electron diffusion theory, as presently formulated, can only account for negative charging, and there is now ample evidence that positive charging, as well as negative charging, occurs on rocket motors. A reappraisal of the charging mechanisms and the above analysis is, therefore, obviously in order.

It is apparent, for example, that a lower electron density in the combustion plasma would contribute to a longer life for charged particles injected into the plasma. The typical values given above for the combustion chamber do not apply to the nozzle exit plane. At the exit plane, the electron density may be as low as 10^9 cm^{-3}. Although the collision frequency will also be reduced at the exit plane, the net change in electronic and ionic conductivity may be 1-to-2 orders of

magnitude. The distance travelled by a positively charged particle before it is neutralized may therefore vary from several tenths of a meter to as much as a few meters. If the particle is injected near the exit plane, therefore, it may effectively escape before it is neutralized. Even with such an increase in discharge time, however, negative particles would be effectively discharged before they have moved more than a few millimeters. Hence, this consideration makes negative charging (by ejection of positively charged particles) by mechanisms other than electron diffusion appear feasible, but it does not make any of the positive charging mechanisms acceptable.

It is also important to recognize that the discharge time computed from Eq. (6) does not take into consideration the motion of the ionized gas. For a particle in the combustion chamber, this motion would not be important. Near the rim of the nozzle, however, all of the neutralizing current must flow upstream to reach the nozzle. If the flow velocity is greater than the drift velocity of the electrons or ions under the influence of the field produced by the charged particle, the particle cannot be neutralized. The drift velocity of an ion under the influence of an electric field E is

$$v = KE \tag{7}$$

where K is the ion mobility given by $K = e/\nu_i M$. For a positive ion at the exit plane, the mobility is of the order of 10^{-4}, and for an electron at this location the mobility is of the order of 10^{-1} m^2/volt-second. An exit velocity v meters per second in the boundary layer thus corresponds to a field strength of $10^4 v$ V/m for positive ions and 10v V/m for electrons. That is, if the field strength in the region between the charged particle and the vehicle falls below these values, some of the charge associated with the particle will be removed by the windstream.

Consider, for example, an electron or ion that is created near the rim of the nozzle. The maximum free space field at the nozzle (on a neutral vehicle) is $e/2\pi\epsilon_o r^2$ due to the charged particle. If this field is less than the "wind field" v/K, the particle can escape. The

escape distance r and the "escape time" r/v can thus be computed as a function of the wind velocity. Some typical values of escape distance and escape time are shown in Table IV for wind velocities ranging from 0.2 to 200 m/sec (i.e., from 10^{-4} to 10^{-1} times the typical midstream exhaust velocity). It is interesting to note that the escape distance is generally larger than the ion mean free path at the exit plane (about 10^{-8}m), but that it is generally equal to or less than the Debye length about 4×10^{-5}m). The latter fact is of particular significance in the positive charging mechanisms, since it indicates that an electron reaches its escape distance while it is still in the positive ion sheath. Because the sheath is a region partially depleted of electrons, the electronic conductivity of this region is low, and the discharge time is longer. Furthermore, the sheath field will accelerate the electron away from the surface of the nozzle unless the emission rate is so large that the sheath is collapsed. Assuming the sheath is not perturbed by the electron emission, the sheath field would be of the order of 10^3 volts/m and would correspond to a wind velocity of 100 m/sec. The electron escape time ($r/v \approx 10^{-8}$sec) would thus be less than the discharge time (approximately 10^{-6}sec) computed from Eqs. (4) and (6) assuming midstream nozzle exit conditions.

Table IV

THE ESCAPE DISTANCE, r, AND THE ESCAPE TIME, r/v, OF ELECTRONS AND IONS IN THE NOZZLE WIND STREAM

Wind Speed v (m/sec)	Positive Ions		Electrons	
	Distance r (m)	Time r/v (sec)	Distance r (m)	Time r/v (sec)
0.2	1.2×10^{-6}	6×10^{-6}	3.8×10^{-5}	1.9×10^{-4}
2	3.8×10^{-7}	1.9×10^{-7}	1.2×10^{-5}	6×10^{-6}
20	1.2×10^{-7}	6×10^{-9}	3.8×10^{-6}	1.9×10^{-7}
200	3.8×10^{-8}	1.9×10^{-10}	1.2×10^{-6}	6×10^{-9}

A similar model can be constructed to consider the effect of triboelectric charging at the rim of the nozzle. In the case of particles,

however, it is hypothesized that the particle velocity is essentially midstream velocity and that the particle penetrates the boundary layer, strikes the wall, and deflects off the wall with little change in velocity. Then the escape distance is determined from the wind velocity in the boundary layer, but the "escape time" is determined by the particle velocity. Table V lists the escape distance and escape time for various wind speeds assuming a particle velocity of 2000 m/sec. A particle charge of 10^6 electronic charges was assumed. Because of the larger particle charge, the escape distance is 3 orders of magnitude greater than for electrons or ions. Because of the higher particle velocity assumed, however, the escape time for negative particles is comparable to the discharge time computed from midstream conditions.

Table V

THE ESCAPE DISTANCE, r, AND ESCAPE TIME, r/v_p,
FOR PARTICLE SPEED v_p = 2000 m/sec,
AND PARTICLE CHARGE $q = 10^6 e$ (NEGATIVE)

Wind Speed v (m/sec)	Positive Particle		Negative Particle	
	Distance (m)	Time (sec)	Distance (m)	Time (sec)
0.2	1.2×10^{-3}	6×10^{-7}	3.8×10^{-2}	1.9×10^{-5}
2.0	3.8×10^{-4}	1.9×10^{-7}	1.2×10^{-2}	6×10^{-6}
20	1.2×10^{-4}	6×10^{-8}	3.8×10^{-3}	1.9×10^{-6}
200	3.8×10^{-5}	1.9×10^{-8}	1.2×10^{-3}	6×10^{-7}

Although this is only a rough analysis, it appears to support the postulate that electrons emitted from the aft end of the nozzle can escape. It neither proves nor disproves the postulate that triboelectric charging can be an effective positive charging mechanism. Although electron emission may at first appear to be the more promising mechanism, it should be pointed out that electron removal is postulated on

(1) The electrons being emitted at the rim of the nozzle, and.

(2) The emitted electrons being carried away by the windstream in the boundary layer, perhaps with the aid of the sheath field, within a sheath thickness of the nozzle surface.

But if an electron in the sheath can be carried away by the windstream, cannot the positive ions in the sheath also be carried away by the windstream? And because there are many more positive ions than electrons in the sheath, will the net charge removed not be positive? Indeed, this is the basis of the electron diffusion theory for negative charging! In order for electron emission to lead to the removal of negative charge, the electrons must be emitted in sufficient amounts to collapse the ion sheath and form an electron sheath at the nozzle exit. Electron emission in such copious amounts in the region does not seem to be very likely.

Although the possibility of a charged smoke particle escaping the vehicle before it is discharged is still questionable, it appears to be a more promising mechanism for removing negative charge than electron emission. This is because the particles (are assumed to) move at a greater velocity than the ion sheath, and because each particle removes a relatively large charge. Under the appropriate triboelectric conditions, this mechanism could also be an effective mechanism for removing positive charge. In fact, triboelectric charging may well be responsible for both the positive and the negative charging observed in motor charging experiments. The electron diffusion mechanism appears to be valid for the removal of positive charge; but because it postulates the removal of a part of the positive ion sheath with the boundary layer gas flow, sheath thickness is an important parameter in the theory. In motors having exit-plane electron densities of the order of $10^{10} cm^{-3}$, the sheath thickness is of the order of 5×10^{-5} meter or 0.2 mil. Considering the surface roughness of the nozzle, one questions whether or not the boundary layer gases can remove a significant portion of the sheath.

Having computed typical conductivities, discharge times, escape distances, and escape times, one can also comment on some of the other proposed charging mechanisms. Because of the high-conductivity of the plasma, it was deduced that any mechanism for removing negative charge from the vehicle would have to produce the negative charge near the exit-plane in order for the charge to be removed before it was

neutralized. Conversely, any mechanism that produces negative charge only in the combustion chamber cannot be very effective in charging the vehicle, because the charge produced in the combustion chamber will be neutralized before it is removed from the vehicle. Thus charging from fuel flow and atomization and photoelectric or thermionic emission within the combustion chamber cannot be very effective sources of charging. It also matters not that some of the emitted electrons may attach to neutral molecules to become less mobile negative ions; there are adequate free electrons available to support the high electronic conductivity, and it is because of this conductivity that the charge is neutralized. (The negative ion need not be driven to the chamber walls or combined with a positive ion; it need only drive one of the very mobile free electrons to the wall to be completely neutralized insofar as its motor charging capability is concerned.)

One other mechanism, contact charging, that has been proposed as a contributor to the removal of positive charge, would appear to be effective only near the nozzle exit-plane. For it to be effective at all, the ion produced by contact ionization would have to be produced at the combustion chamber (or nozzle) wall. If the ion were produced within the combustion gases by, say contact with a suspended hot particle, no net charge would be carried away by the exhaust gases, since both the positive ion and the electron-bearing contacted particle would be exhausted. If the ion were produced by contact with the walls it would be created in the positive ion sheath and would only enhance the ion density in the sheath. In the sheath it would also be under the influence of the sheath field which tends to force the ion back to the wall. At the aft end of the nozzle, where a part of the sheath is presumably carried away by the windstream, contact ionization might be effective in enhancing positive ion removal if contact ionization could occur in this region. Contact ionization requires a rather special relationship between the contacting atom and the contacted surface. The removal of positive charge by other mechanisms seems quite possible, so further consideration of the contact ionization mechanism does not seem warranted.

B. Vehicle Potential

The charging considerations thus far have been predicated on the assumption that the vehicle potential is zero. Because the vehicle potential immediately assumes a nonzero value if charging occurs, a more practical consideration may be the effect of vehicle charging on vehicle potential. If the vehicle potential is limited to a few volts, for example, fairly large short circuit currents would be tolerable; if, on the other hand, the vehicle potential can attain values greater than the corona threshold potential, even relatively small charging rates will be of concern. It is therefore important to examine some techniques that might be used to estimate the limitations that can be placed on the vehicle potential.

In the lower atmosphere, where the motion of charge carriers (electrons and ions) is controlled by collisions with neutral molecules, the velocity of the carrier under the influence of the electric field E about the charged vehicle is KE, where K is the mobility of the carrier. When the drift velocity due to the electric field is equal to the wind velocity that is attempting to carry the particle away from the vehicle, the net velocity of the particle relative to the vehicle is zero, and charging ceases. That is, when

$$KE = v_w \tag{8}$$

the vehicle potential will approach an equilibrium value at which charging stops, or at which the electric field captures charge from the exhaust at the same rate that the exhaust expels charge. Since the electric field E at any point on the vehicle is directly related to the vehicle potential, it is, in principle, possible to determine the equilibrium potential of the vehicle.

The relation between the vehicle potential and the electric field strength can be obtained quite easily by modeling techniques such as those described in Refs. 1 and 2. The principal difficulty will be in ascertaining the region of the vehicle at which the field should be determined and in evaluating the velocity pertinent to this analysis.

It can be presumed that the region of interest will be the aft end of the nozzle on metal-nozzled rockets, and the velocities of concern are the velocities in the boundary layer and wake aft of the nozzle rim. Both the electric field and the gas velocity exhibit strong spatial dependence in the vicinity of the nozzle rim. In reality, therefore, the drift velocity KE and the gas velocity v_g in Eq. (8) should be integrated over the regions of the nozzle where current is being captured by the electric field and the region where charge separation is occurring because of gas motion. For the purpose of demonstrating the application of this theory, however, an effective electric field and an effective gas velocity will be assumed. Letting the effective field strength be $k_e V$ and the gas velocity in the boundary layer be $K_v g I_{sp}$, the equilibrium potential of the vehicle will be

$$V = k_v g I_{sp} / k_e K \qquad (9)$$

where gI_{sp} is the effective exhaust velocity determined from the gravitational constant g and the specific impulse I_{sp}, and k_v is the ratio of the boundary layer velocity to the effective exhaust velocity.

For the Nike-Cajuns, the field strength at the field meter was about 3 times the vehicle potential. The field strength at the nozzle rim will be much higher than the field on the cylindrical surface--perhaps 30 times as high. Therefore, k_e may be of the order of 100. The gas velocity gI_{sp} is about 2000 m/sec, but near the nozzle wall, the velocity will be considerably less. Let us assume that k_v is of the order of 10^{-1}. The ion mobility at the exit plane at sea level is of the order of $10^{-4} m^2$/volt-second. The equilibrium potential computed from Eq. (9) using these values is thus 2×10^4 volts. This order of magnitude estimate of the equilibrium vehicle potential is within a factor of 2 of the maximum vehicle potentials measured on the Nike-Cajuns and Viking at low altitude!

Although the agreement between the measured values and the computed value is undoubtedly fortuitous, the estimated values of k_e and k_v are believed to be representative. It is noted, however, that the ion mobility was used in computing the vehicle potential rather than the

electron mobility. Had the electron mobility been used, the vehicle potential would be three orders of magnitude lower, and, therefore three orders of magnitude different from the measured potentials. Thus ion mobility, rather than electron mobility, appears to lead to more realistic values of vehicle potential in Eq. (9). Even though electrons are abundant in the exhaust gases, these electrons may become attached to gas molecules in the mixing zone aft of the nozzle rim. Thus negative charge collected by a positively charged vehicle may be in the form of negative ions rather than free electrons.

At 10 kilometers where the Cajun engine ignited, the collision frequency is about 1/3 the sea level value, so that the ion mobility is increased by a factor of 3 and the vehicle potential is reduced by a factor of 3 to about 7 kilovolts. This is somewhat higher than the observed value of about 2 kilovolts during Cajun burning. There are other differences between the sea level burning of the Nike and the 10 kilometer burning of the Cajun, however. The geometry of the nozzle has considerable influence on the field strength in the vicinity of the nozzle; therefore the value of k_e appropriate to the Nike nozzle is not necessarily applicable to the Cajun nozzle. Because the Cajun is smaller in diameter than the Nike, it would not be surprising if the value of k_e (the field strength per volt of vehicle potential) were higher for the Cajun than for the Nike. (A larger k_e would reduce the equilibrium potential.)

At high altitudes, where the ambient mean free path is of the order of the vehicle dimensions, electrons or ions may be drawn directly from the edge of the exhaust plume to the motor case with virtually no collisions with neutral molecules. Energy considerations can then be used to determine the vehicle potential, since no energy is lost by the ion in collisions with other molecules. The energy imparted to an ion ejected by the exhaust is $mv^2/2$. On the average, however, the ion cannot escape the vehicle unless its energy exceeds eV, where V is the vehicle potential. Thus an equilibrium potential is reached when

$$eV \approx mv^2/2$$

or

$$V \approx mv^2/2e \qquad (10)$$

Using an ion mass of 28 AMU and the full exhaust velocity of 2000 m/sec, the vehicle potential deduced from Eq. (10) is only 0.54 volts. If the electron mass were used in Eq. (10) (attachment should not occur very rapidly at these pressures), the vehicle potential would be four orders of magnitude lower. Unfortunately, there are no experimental data available for comparison with these results.

It is noted that the effect of an ion sheath that might be formed about the vehicle in the ionosphere has been neglected in deriving Eq. (10). Because of the extremely low vehicle potentials predicted by Eq. (10), it is doubtful that one could discriminate without considerable effort, between the vehicle potential produced by engine charging and the normal wall potential an inert vehicle acquires in the ionosphere.

V CONCLUSIONS AND RECOMMENDATIONS

It was point out in Section I B that rocket engine charging was anticipated to have one of three effects on vehicle performance:

(1) It could charge the vehicle to potentials above the corona threshold, thereby producing electromagnetic interference in the onboard systems,

(2) It could charge the vehicle to potentials below the threshold potential but high enough to cause interstage sparking between isolated stages or rendezvousing vehicles, or

(3) The rocket exhaust could act as an effective discharger to maintain the vehicle potential at a relatively low value.

No available experimental data indicate that the first possibility is very likely on rocket motors, but it is known to be a common effect of jet engine charging. The difference between jet engine behavior and rocket engine behavior is undoubtedly due to the higher conductivity of the rocket engine exhaust.

The experimental data indicate that effect (2) will be applicable at low altitudes. Vehicle potentials from 17-to-40-kilovolts have been observed on small sounding rockets at altitudes below 10,000 ft. It is presumed that similar potentials (perhaps scaled up with vehicle size) will be observed on larger launch vehicles. In order to ascertain the validity of this presumption, however, it is recommended that a number of the larger launch vehicles be instrumented with field meter systems similar to the one used on the second Nike-Cajun so that vehicle potentials during launch can be measured.

The experimental data also indicate that effect (3) will be applicable at higher altitudes. The exact altitude range at which the engine becomes an effective discharger has not been determined, but the Nike-Cajun data indicate that the vehicle potential is limited to a few kilovolts at altitudes of the order of 45,000 ft. Whether the larger

rocket engines will be as effective at this altitude is not known. It is also not known what effect moderate-to-heavy precipitation charging will have on the vehicle potential when the engines are operating. Further flight data are required to provide information on the variation of potential with altitude and on the ability of the plume to discharge the vehicle in the presence of precipitation charging.

Because of the conductivity of the exhaust plume, it also appears that excessive differences in potential between sections of the vehicle during staging cannot exist if the upstage motor is ignited at the time of staging. As long as the expended stage is contacted by the ionized exhaust of the active motor, the two will be electrically connected and at approximately the same potential. If staging occurs before the upstage engine is ignited, and if the vehicle is charged to a high potential, a difference of potential can be developed as separation increases. This potential difference does not assume significant proportions, however, unless the vehicle was charged to a very high potential before separation, or unless the separated sections are very far apart. Evidence available at present suggests that the vehicle potential at staging altitudes will be quite small, so that the first condition is not met. A sizeable potential difference under the second condition is of no particular consequence because of the large separation between the sections required to develop the potential difference. If staging occurs above 60 kilometers, it is anticipated that the vehicle will not have a significant potential before separation and that the ionosphere will maintain both sections of the separated vehicle at very low potentials regardless of how far apart they are removed.

Additional experimental data are needed to ascertain the behavior of rocket motors in the ionosphere and in space. No experimental data are available to the systems engineer from vehicles whose engines are active in the ionosphere. It is anticipated on the basis of laboratory experiments, theory, and high altitude flight data, however, that vehicle potentials in the ionosphere and in space will be extremely small. Such potentials would probably be of importance only to special experiments, such as mass spectrometer or ion energy experiments, in which vehicle

potential affects the interpretation of the experimental data. Because of the serious consequences to rendezvousing spacecraft of underestimating the effect of engine charging and the ease with which the experimental data can be obtained, it is recommended that steps be taken to measure the vehicle potential on a vehicle whose engines operate in the ionosphere.

As indicated in Section IV, additional data are also needed on the electrostatic behavior of some of the more or less special vehicle configurations such as those that are coated with insulating heat shields or ablative material, and those that use insulating nozzles. No experimental data are available for these vehicles, and engine charging theory is not sufficiently developed to reliably predict the effect of these factors on the vehicle charging characteristics. The only basis for evaluating the characteristics of these vehicles that is available at present is the fact that many vehicles of this type have been launched with no evidence of electrostatic effects clearly attributable to engine charging.

The state of development of engine charging theory remains relatively primitive even for metal-skinned rockets with metal nozzles. At present, charging theory is better suited to excluding proposed charging mechanisms than it is to ascertaining charging rates or vehicle potentials. It appears that several mechanisms for negative charging (positive charge removal) are possible, for example, but most of the mechanisms proposed for positive charging appear to be excluded. Triboelectric charging due to solid particles in the exhaust appears to be the most promising mechanism for positive charging, but there is no incontrovertible evidence that this is the mechanism. It is anticipated that the development of engine charging theory will benefit from further experimental data from both flight vehicles and laboratory experiments.

ACKNOWLEDGMENTS

The authors acknowledge with gratitude the support and assistance of the following who contributed to this program: Mr. J. B. Chown, Mr. W. C. Wadsworth, Mr. J. R. Woodbury, Mr. S. T. Dixon and Mr. W. C. Wong. Mr. Chown and Mr. Wadsworth were instrumental in getting the short circuit current measurements incorporated in the original static firing program. Mr. Wadsworth also assisted in instrumenting and performing the open-circuit voltage measurements during the second series of static firings. Mr. Woodbury designed the electronic circuits used in the second Nike-Cajun field meter system, and Mr. Wong fabricated, tested, and calibrated the field meter system for this experiment. Mr. Wong also performed the laboratory measurements on the Nike-Cajun models to determine the electrostatic properties of the rocket. Mr. Dixon assisted in instrumenting and performing the ethylene-oxygen flame experiments.

Appendix A

MEASUREMENTS OF SHORT CIRCUIT CURRENT FROM STATIC FIRINGS

Appendix A

MEASUREMENTS OF SHORT CIRCUIT CURRENT FROM STATIC FIRINGS

1. Solid Fuel Motors

The initial experiments on rocket motor charging were conducted to measure short-circuit charging current. Since, at the time of these experiments, there was limited support for studies of vehicle electrification problems on rocket vehicles, the experiments were conducted on a "piggy back" basis with experimental studies of optical and microwave properties of rocket motor exhausts during static firings being conducted under Contract NAS7-179.[7] To measure short circuit charging currents, it was necessary only to insulate the motor from its grounded supporting structure and make the ground connection through a galvanometer. This modification of the test facility was inexpensive and did not compromise the primary experiments. Hence, although the short circuit charging current is perhaps not the most useful motor charging parameter, it appeared to be easily obtained and represented a first step toward the determination of rocket charging characteristics.

The motors used in these experiments were 5-inch-diameter solid fuel motors containing a basic fuel of medium-burning-speed polyurethane and ammonium perchlorate seeded with potassium. The basic fuel mix contained 20 percent polyurethane, 79 percent ammonium perchlorate, and 1.0 percent potassium chlorate by weight. An aluminized version was also prepared by substituting 15 percent aluminum for a like amount of ammonium perchlorate. The fuel was cast in a steel motor case and fitted with a 0.70 inch diameter graphite throat and steel expansion nozzle. The motor assembly is illustrated in Fig. A-1. The motors were mounted with their axes horizontal in the test bay and fitted with the hard glass isolation section and the steel diffuser tube. Burning time for these motors was about 5 secs.

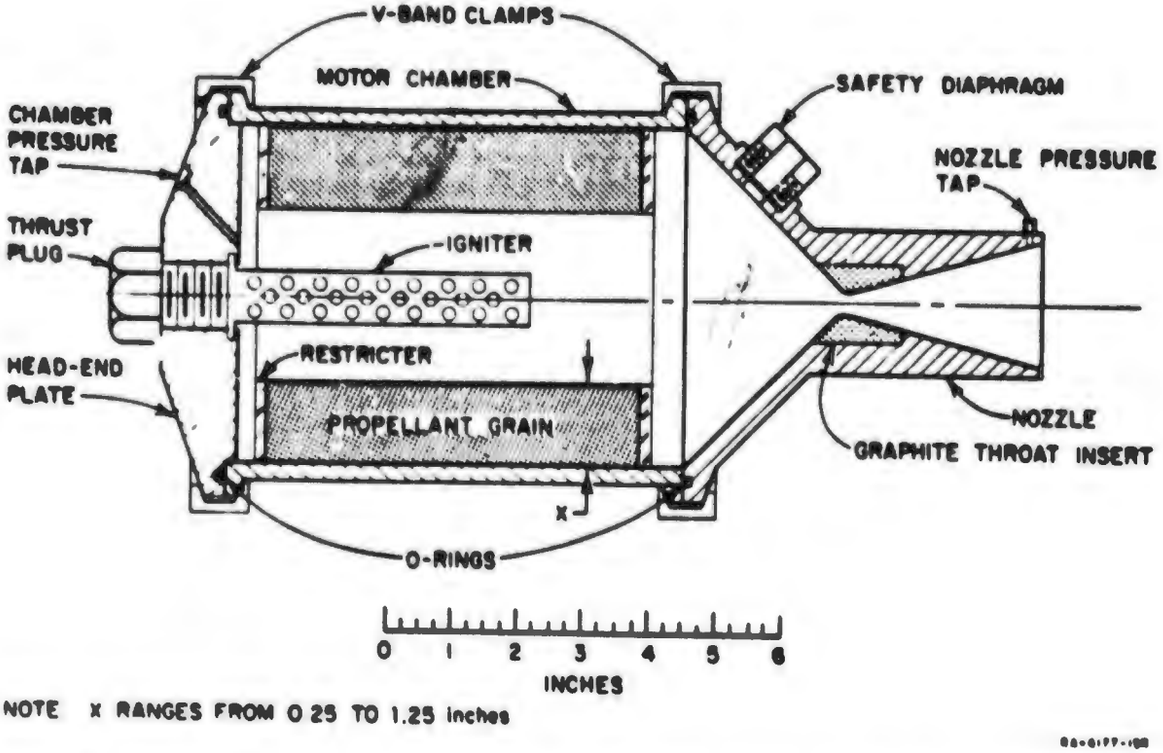

FIG. A-1 CONSTRUCTION OF 5-INCH MOTORS USED IN STATIC FIRINGS

For the primary experiments conducted on these motors, a low exit plane pressure was desired to simulate a high altitude mode of operation. Hence, a special exhaust system had been devised so that the exhaust gases flowed through a 45-inch-long steel pipe that was connected to the motor exhaust nozzle through an 8-inch-long hard glass pipe (see sketch in Fig. A-2) so that the exit plane pressure was about 1.5 psia. Both the glass pipe and the steel diffuser pipe were approximately 3-1/4 inches, inside diameter. Since the 45-inch steel pipe was electrically isolated from the motor through the glass pipe, and was isolated from ground, provision was made to ground it through a second galvanometer on the recorder. Thus, the charging rates to both the motor and the steel diffuser tube were measured.

The charging currents to the motor and diffuser tube are shown in Fig. A-2 for the potassium seeded (non-aluminized) motor. In this illustration, as in all illustrations in this section, zero time is taken at the beginning of chamber pressure rise, since there was a variable delay of several seconds from the time the ignitor was energized

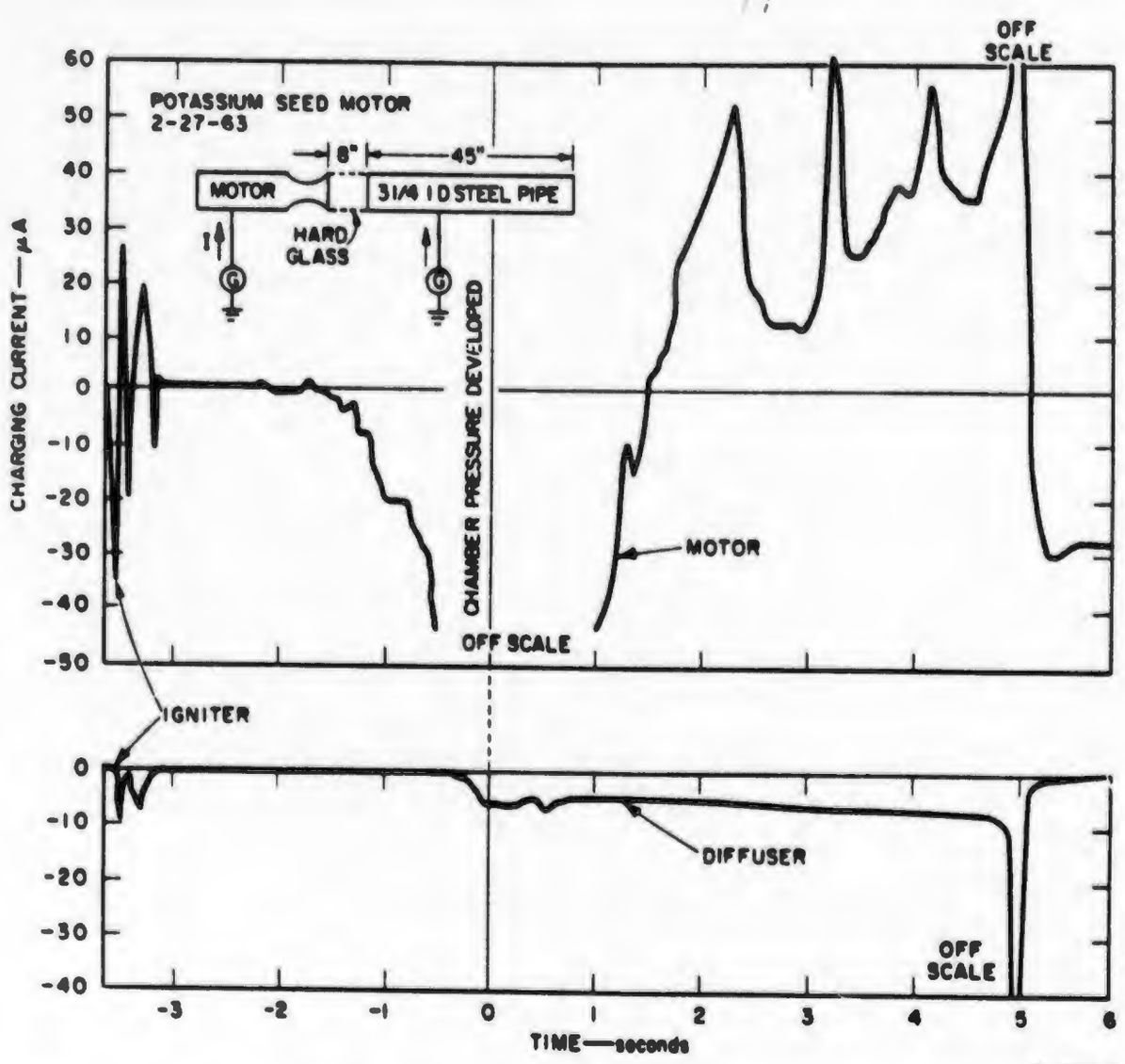

FIG. A-2 MOTOR AND DIFFUSER CHARGING CURRENTS FROM 5-INCH SOLID FUEL MOTOR

until the propellant ignited and developed chamber pressure. Igniter activity was accompanied by a burst of erratic charging between -4 and -3 sec which is prominent in Fig. A-2 in both the motor and the diffuser charging currents. Once the igniter transient had subsided, there was little charging activity until about one second before pressure build-up. At this time, the motor charging current increased in the negative direction (i.e., positive charge was flowing from the motor to ground through the galvanometer) until the galvanometers were driven off scale. As the chamber pressure built up and the combustion activity stabilized, the motor charging current reversed sign and varied from 10 to 60 μamp until a fraction of a second before burnout, when the galvanometer was driven off scale on the positive current side (motor being charged negatively). From pressure build-up until slightly before burnout, the diffuser appeared to charge at a fairly uniform rate independently of the motor. Just prior to burnout, however, a sharp increase in the diffuser current is noted which appears to be related to the increase in the motor charging current at this time. The polarities of the motor and diffuser charging currents at this time are such that the diffuser current could be interpreted as a circulating component of current flowing through the loop formed by the galvanometers, ground, and the plasma of the exhaust gases between the motor and the diffuser. It is also of interest to note that after burnout, the motor charging current did not immediately return to zero, although it gradually returned to zero several minutes after burnout.

The second motor fired was one of the aluminized motors. Since it was anticipated that the aluminized motor would produce higher charging rates than the nonaluminized motor described above, the galvanometer sensitivities were reduced. In spite of the reduced sensitivities, the diffuser charging current was off scale (over 120 μamp) during most of the motor burning period. Figure A-3 shows the motor charging current for the aluminized motor. The igniter transient was again prominent, and the initial negative current in the vicinity of chamber pressure build-up is similar to that obtained with the nonaluminized motors.

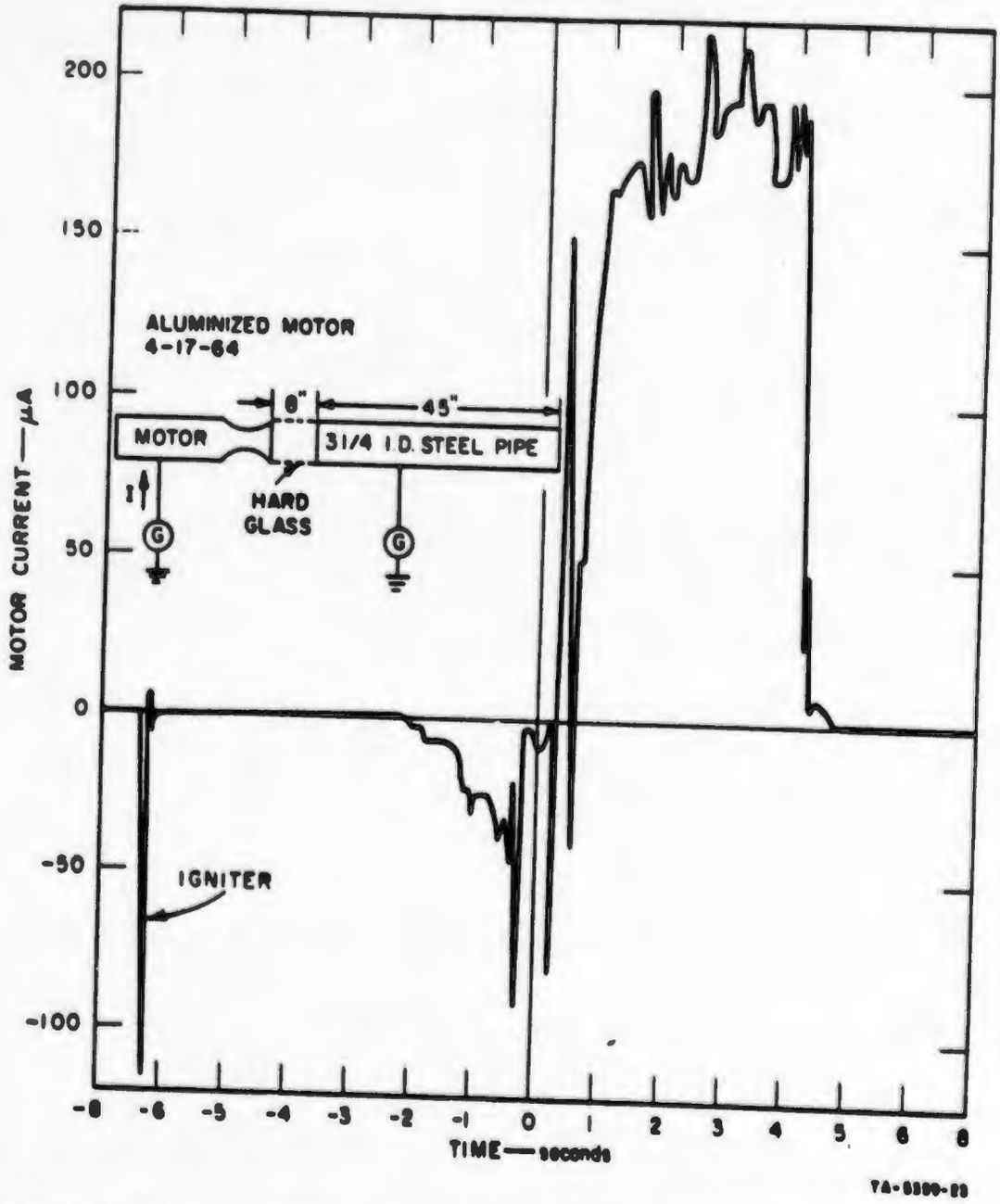

FIG. A-3 MOTOR CHARGING CURRENT MEASURED ON ALUMINIZED MOTOR

As was anticipated, the charging currents for the aluminized motor were much higher than for the nonaluminized motor.

Since the diffuser current drove the galvanometer off scale during the motor burning period, it was not possible to compare the diffuser current with the motor current. On studying the data for the two-second period prior to pressure build-up, however, it was observed that the diffuser current was almost equal in magnitude, but opposite in polarity, to the motor charging current. This relationship is illustrated in Fig. A-4, which shows a reproduction of the strip chart data for the two-second period prior to pressure build-up. Careful study of these data indicate that the diffuser current is actually about 10 percent greater in magnitude than the motor current. It is apparent, however, that the current circulating in the loop formed by the galvanometers, ground and exhaust plasma predominates over any net charging current to either the motor or the diffuser. At burnout, when the diffuser current came back on scale, a similar relationship between motor current and diffuser current was observed.

Prior to firing the third motor, the galvanometer sensitivities were again reduced in an effort to obtain the diffuser charging current. When the third motor, which was also aluminized, was fired, however, both the motor and diffuser galvanometers were driven off scale, indicating that currents in excess of 1000 μamp were produced. Although both galvanometers were driven off scale within 30 msec after the beginning of the motor chamber pressure rise, it was apparent that the motor current and diffuser current were of opposite polarity. Furthermore, the motor current was negative (according to the convention established in this section), rather than positive as had been observed in the previous aluminized motor firing. After burnout (i.e., depressurization of the combustion chamber), charging of the motor and diffuser continued for about one second at on scale levels. A reproduction of the charging current data for this period is shown in Fig. A-5. It is apparent from Fig. A-5 that the motor and diffuser currents were again predominantly circulating currents even in this post-burning period. Depressurization

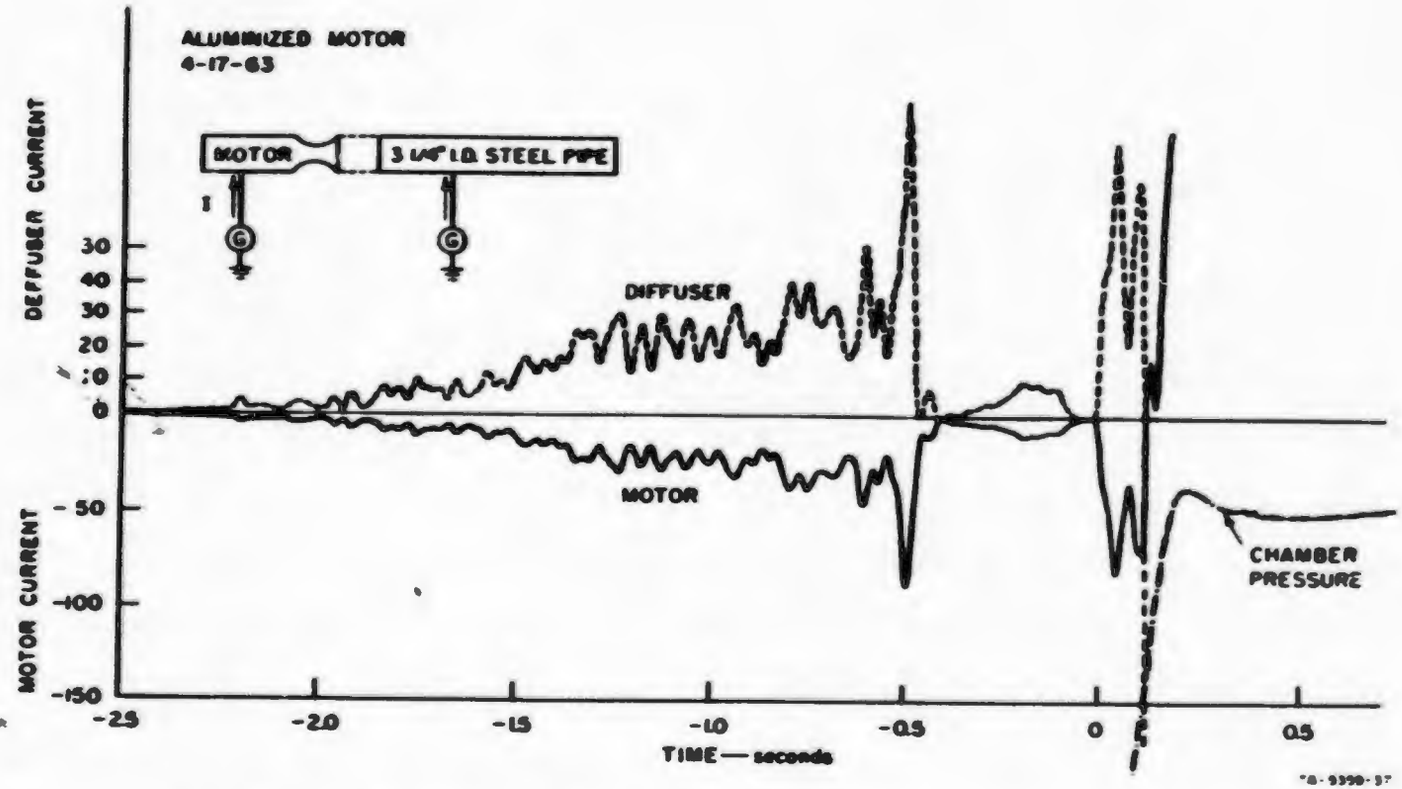

FIG. A-4 MOTOR AND DIFFUSER CURRENTS PRECEDING CHAMBER PRESSURIZATION ON ALUMINIZED MOTOR

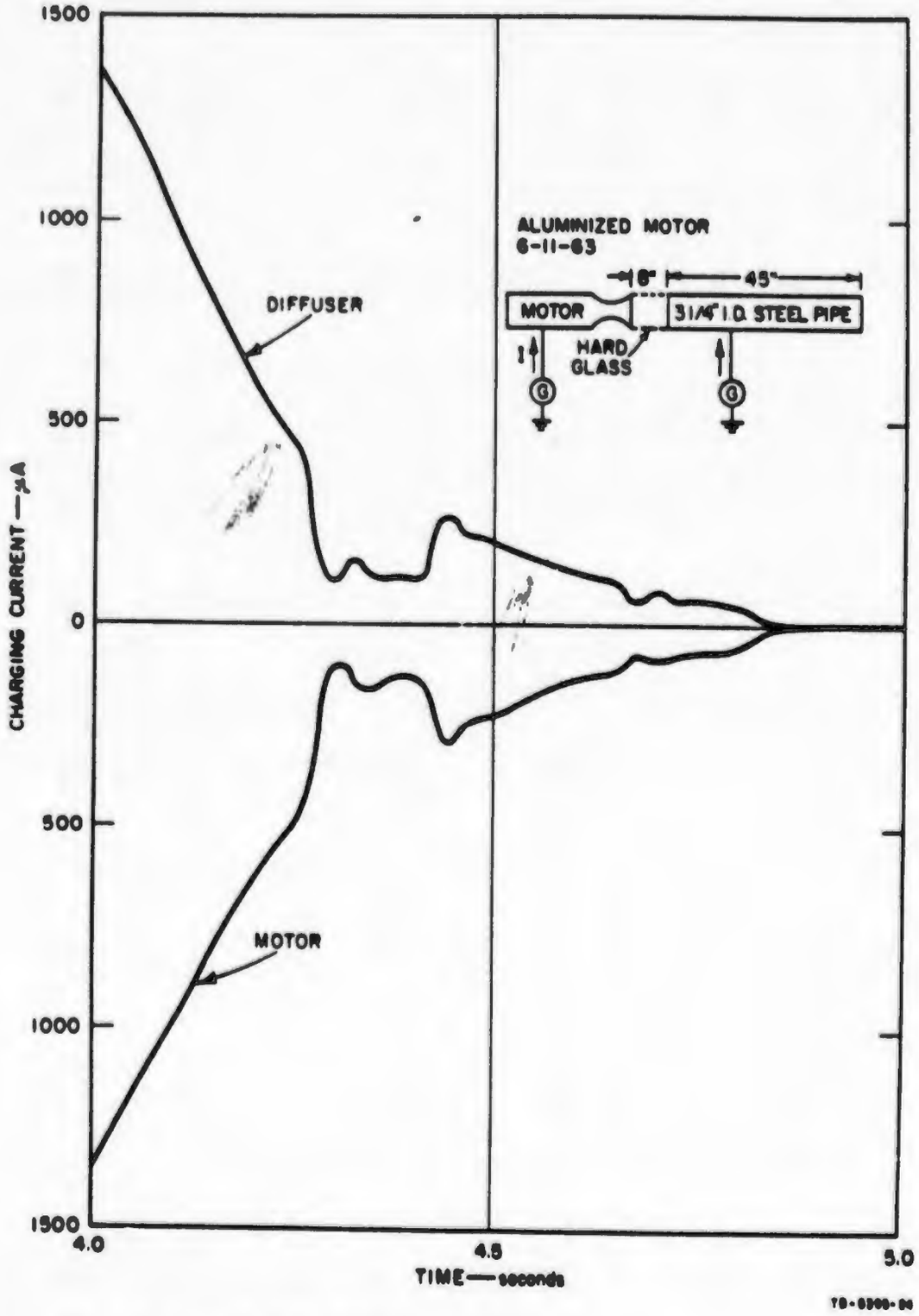

FIG. A-5 MOTOR AND DIFFUSER CURRENTS DURING BURN-OUT OF SECOND ALUMINIZED MOTOR

of the chamber began at 3.72 sec and was complete at 3.89 sec after the beginning of chamber pressure build-up.

The characteristics of the third motor also differed from those of the previous two motors in that this motor exhibited no charging prior to the beginning of chamber pressure build-up. As is illustrated in Fig. A-2 and A-3, the igniter squib produced charging activity in the earlier firings, and considerable charging activity was observed over one second before significant chamber pressure was observed.

The general characteristics of the three motors fired in these experiments are given in Table A-1. The burning time given in the table is the time between the beginning of chamber pressurization and the end of

Table A-1

MOTOR CHARACTERISTICS

	Motor 1 2-27-63	Motor 2 4-17-63	Motor 3 6-11-63
Fuel	Basic Fuel	Aluminized	Aluminized
Burn Time (seconds)	5.37	4.5	3.89
Electron Density (cm^{-3}) (exit plane)	$<10^9$	$6.5\text{-}24 \times 10^9$	$6.5\text{-}24 \times 10^9$
Motor Charging Current (μamp)	10-60 pos.	160-210 pos.	>1000 neg.
Diffuser Charging Current (μamp)	6-35 neg.	>120 neg.	>1000 pos.
Max. Chamber Pressure (psi)	330	420	485
Throat Diameter (inch)	0.70	0.70	0.70

depressurization. The electron densities at the exit plane were obtained with a microwave interferometer at the hard glass isolation section between the motor and diffuser. With the basic fuel, the electron density was too low to be accurately measured, but it is estimated to have been between one and two orders of magnitude less than the electron density for the aluminized motors. The chamber pressure was obtained from a pressure transducer connected to the chamber pressure tap (see Fig. A-1) during the test. The chamber pressure was fairly constant during burning.

3. Experiments with Ethylene Oxygen Burner

Since only three static firings of the 5-inch solid-fuel rocket motors were made in the series of tests described above it was not possible to conduct additional short circuit current measurements on motors of this type. Arrangements were made instead to use a small ethylene-oxygen motor to perform additional experiments in the laboratory. The ethylene-oxygen motor, which was used primarily for experiments to study the electrical properties of the exhaust flame, had the advantage that it could be fired and seeded with very little set-up time. In addition, the fuel mixture and flow rate could be varied during a run, and the motor could be burned continuously for extended periods of time.

The ethylene-oxygen motor is installed in a 4 x 4 x 8 foot metal vacuum chamber equipped with a high-speed mechanical vacuum pump capable of maintaining the pressure at 10 to 20 mmHg while the motor is burning. A schematic diagram of the ethylene-oxygen motor and accessory equipment is shown in Fig. A-6. All access to the chamber for gas lines, water lines are through a port in the base of the chamber. A water-cooled baffle section to cool the hot gases from the flame is inserted in the exhaust line before the 4-inch gate valve which is used for flow control. The vacuum pump, which is located outside the building, is a 200-cfm rotary gas ballast pump. The gas ballast feature of the pump system is necessary because large amounts of water vapor must be handled.

The ethylene-oxygen flame used in the experiment results from the thermochemical reaction

$$C_2H_4 + 3O_2 \rightarrow 2H_2O + 2CO_2 + \text{Heat}.$$

The CO_2 and H_2O subsequently disassociate into CO, H_2, O_2, O and H. This disassociations, which are endothermic, use an enormous amount of heat, which limits the flame temperature. The ethylene gas is used because of its relatively high temperature--about 2,500°K--and ease of handling. The gas flow to the burner is controlled by a nullmatic pressure regulator and jeweled metering orifice.

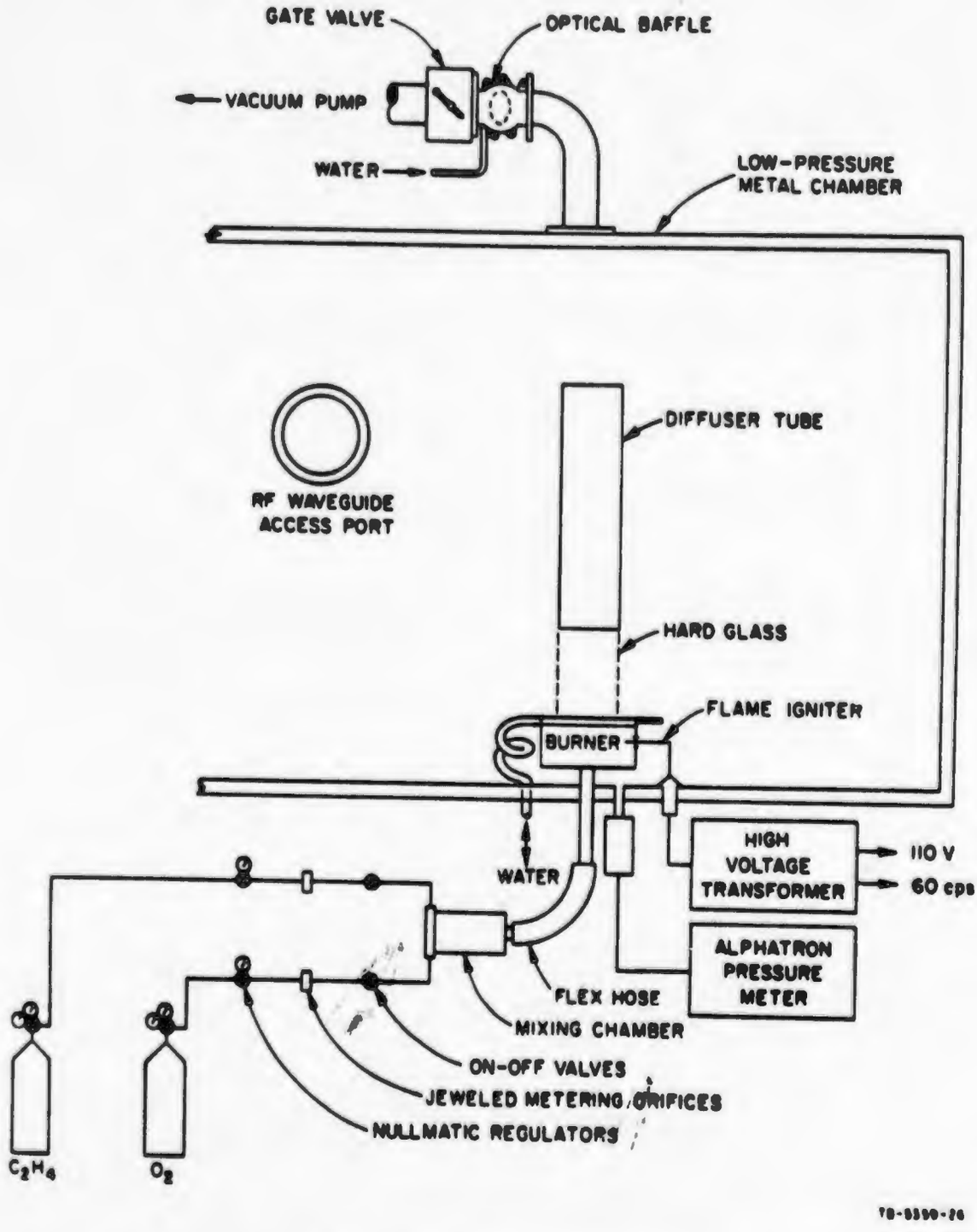

FIG. A-6 APPARATUS FOR CONDUCTING EXPERIMENTS WITH ETHYLENE-OXYGEN FLAME

After the gases are metered they pass to a mixing chamber, which serves also to prevent flow resonances. The premixed gas is then passed to the burner through a flexible hose so that the burner can be raised and lowered while the flame is burning. The burner contains a fine mesh stainless steel screen which acts as a flame arrestor and diffuses the gases so that a uniform velocity exists across the burner surface. The gas mixture is ignited by a glow discharge formed about an electrode in the burner cavity above the screen. The high voltage is supplied from a 60-cycle high-voltage transformer. The flame exhausts through a 0.75-inch diameter orifice in top plate. This plate is water-cooled to prolong the life of the motor nozzle.

To perform the motor charging experiments, the motor was electrically isolated from the grounded chamber walls by mounting the burner on an insulating base and supplying the cooling water through plastic tubing. After the fuel had been ignited, the igniter lead was disconnected so that the motor was not grounded through the igniter circuit. To simulate the diffuser tube used with the solid fuel motors, a brass tube was mounted over the exhaust plume above the burner and electrically isolated from the burner with a section of glass pipe. Provisions were made to measure the charging current to the motor, diffuser, and igniter individually or in any combination.

The initial experiments with the ethylene-oxygen motor were at a vacuum-chamber pressure of 14 mmHg with a fuel rich mixture containing 69 mole percent oxygen and 31 mole percent ethylene. The flow rate for the fuel mixture was about 0.09 liters per second. Currents to the motor, igniter, and diffuser were measured in various configurations, as illustrated in Fig. A-7. In each configuration in Fig. A-7, the magnitude (in microamperes) and direction of the measured current is shown adjacent to the part of the circuit in which the measurement was made. Because of fluctuations in charging characteristics, the values of corresponding currents in two similar configurations such as Fig. A-7(a) and (b) do not agree exactly; however, the general trends of these measurements seem to be consistent.

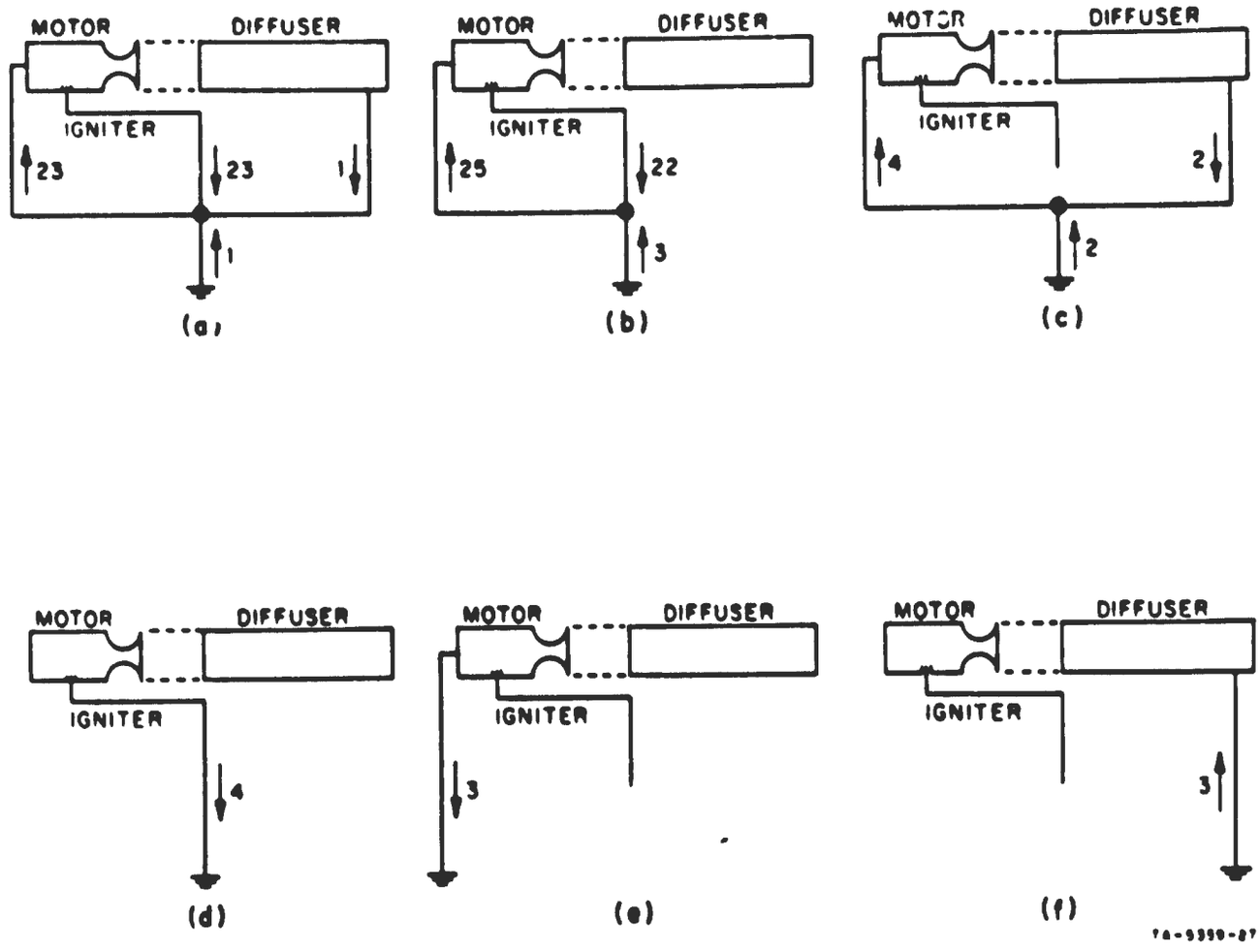

FIG. A-7 MOTOR, DIFFUSER, AND IGNITER CURRENTS MEASURED IN VARIOUS CONFIGURATIONS

If allowance is made for the fluctuations in the currents some conclusions can be drawn from the test results shown in Fig. A-7. From Fig. A-7(a) it is apparent that a large circulating current flows in the igniter-motor loop, since currents of the order of 20 μamp flow in this loop, while the net charging current is only 1 μamp. In the course of these experiments it was noted that the current in the igniter lead was always of such a direction as to suggest that the igniter was emitting electrons. Since the igniter is in the combustion chamber of the motor where its temperature may be quite high, it has been hypothesized that the igniter was thermionically emitting electrons into the combustion chamber plasma to produce the large circulating current. It is interesting to note that this electron emission within the combustion chamber produces only large circulating currents and does not affect the net

charging current to the system. [The net charging current is 1 μamp in Fig. A-7(a).] Thus, on the one hand, the electrons emitted by the igniter are not carried out of the system by the exhaust gases, but, on the other hand, an attempt to measure the motor charging current with the igniter grounded [e.g., as in Figs. A-7(a) and (b)], would lead to a motor charging current an order of magnitude too high.

In Fig. A-7(b), the diffuser was disconnected and allowed to float. Here it is noted that isolation of the diffuser does not appear to have much influence on the current circulating in the igniter-motor loop. The net charging current in Fig. A-7(b) is in the same direction as in Fig. A-7. This again suggests a net collection of electrons by the motor and igniter in Fig. A-7(b), in spite of the apparent emission of electrons by the igniter.

In Fig. A-7(c), the igniter was disconnected and allowed to float. Note that the current in the motor line, which was over 20 μamp when the igniter was connected, was reduced to only 4 microamperes when the igniter was disconnected. Also of interest is the direction of the currents in the motor and diffuser lines in Fig. A-7(c), since the direction of flow suggests that part of the current in the motor line is produced by a circulating current in the diffuser-motor loop.

In Figs. A-7(d), (e), and (f), the three line currents were measured individually with the other lines disconnected and floating. Note that the igniter again appears to be emitting electrons, but the electron current is much lower in Fig. A-7(d) than it is in the cases where an external path is provided for current circulation. Also of interest, is the fact that both the motor and the diffuser collect electrons from the combustion plasma, as would be predicted on the basis of electron diffusion theory, when acting individually as in Figs. A-7(e) and (f). In comparing Fig. A-7(f) with Figs. A-7(a) or (c), however, it is noted that when a loop is formed by connecting the motor line to the diffuser line, the direction of current flow in the diffuser line is reversed. This fact tends to reinforce the validity of the suggestion made above that the diffuser current in Fig. A-7(c) is a circulating component.

To investigate this circulating component further, a variable dc bias supply was inserted in the motor-diffuser loop in the configuration of Fig. A-7(c), and the currents in the motor and diffuser lines were measured. The results of this experiment are shown in Fig. A-8. The shape of these curves is interesting in that the magnitude of the circulating current increases rapidly with increasing positive bias voltages, but is relatively independent of bias voltage for negative bias voltages. This behavior of the circulating current with bias voltage suggests that the diffuser is behaving as a sheath-area limited Langmuir probe, since when the diffuser is negative, it appears to be collecting a saturation ion current, while at positive diffuser potentials large electron currents are collected. For this explanation of the circulating current characteristics to be valid, however, it must be assumed that the motor is not sheath area limited. This would imply that either the electron-ion density at the motor exit plane is much higher than it is in the vicinity of the diffuser, or that the motor is capable of emitting electrons when it is at negative potentials. That the former condition is satisfied is indicated by electron density data obtained from measurements made with a similar motor under similar fuel consumption rates. These data are shown in Fig. A-9. The electron density at the nozzle is an order of magnitude higher than the density 20 centimeters above the nozzle (the approximate height of the lower end of the diffuser). It is also probable that thermionic emission of electrons can occur when the motor is operated for extended periods of time, as it was in these experiments, since the nozzle becomes very hot under these conditions. (A cooling system and periodic shut-down are required to prevent excessive erosion of the nozzle throat.)

Thus, it appears that both a higher electron-ion density and a capability for the emission of electrons exist at the motor exit plane, so that saturation currents for the motor may be several orders of magnitude greater than the saturation current for the diffuser. This being the case, the diffuser current characteristic of Fig. A-8 is probably the Langmuir probe characteristic of the diffuser in the exhaust plasma,

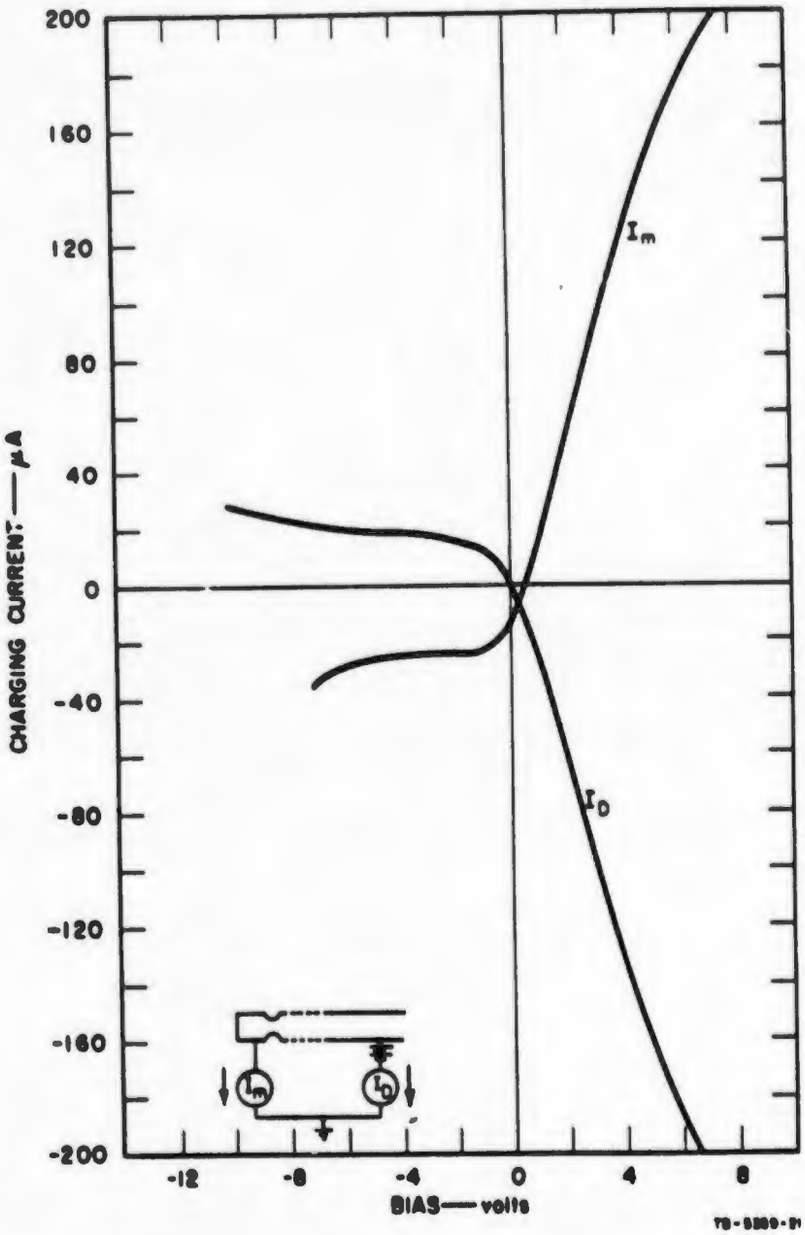

FIG. A-8 VARIATION OF MOTOR AND DIFFUSER CHARGING CURRENTS WITH BIAS VOLTAGE

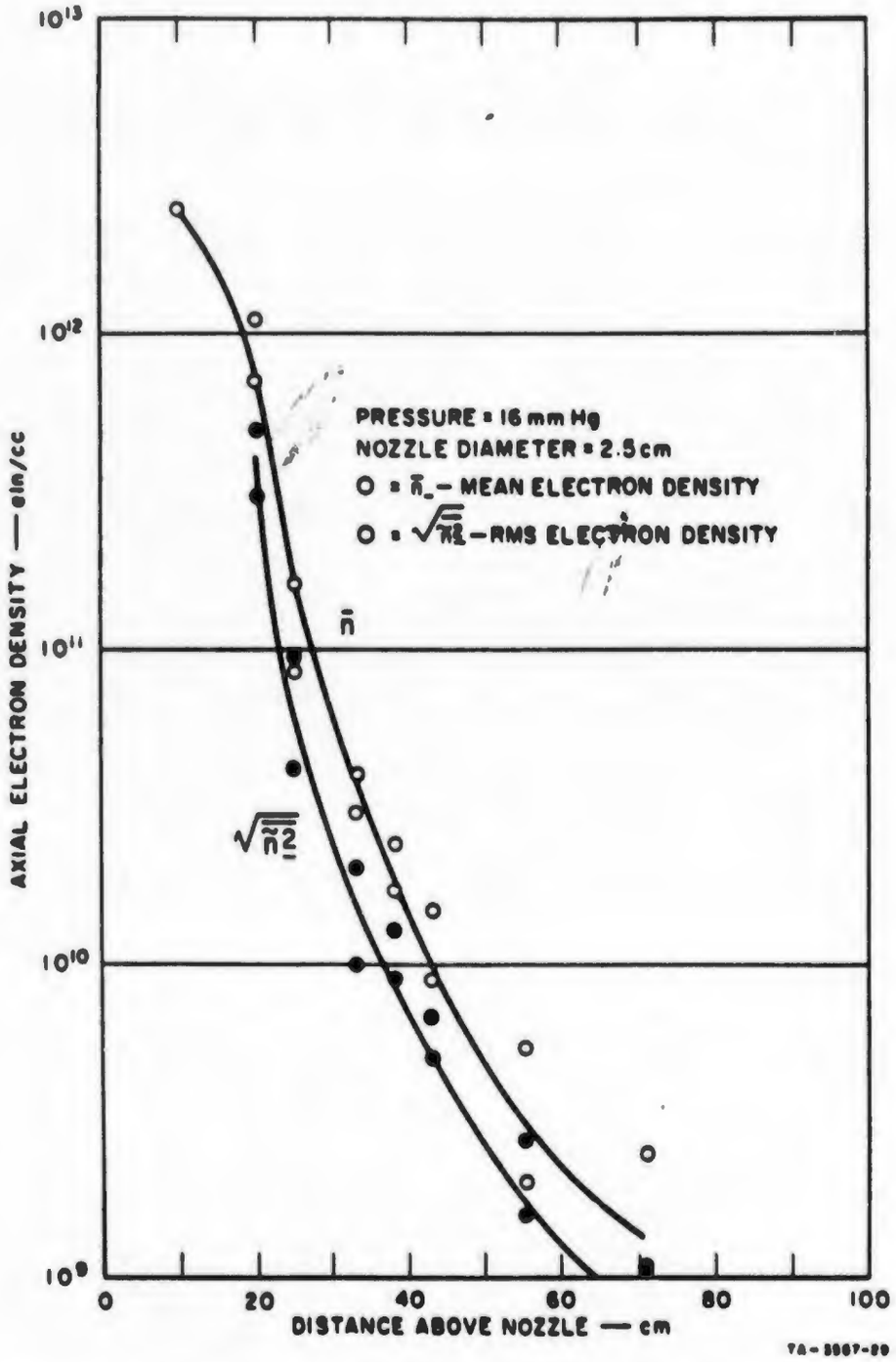

FIG. A-9 VARIATION OF ELECTRON DENSITY WITH HEIGHT ABOVE BURNER IN THE ETHYLENE-OXYGEN FLAME

and the motor current characteristic is simply the diffuser current plus a small net-charging current.

Since the diffuser is capable of collecting current of either polarity with the proper bias, one is inclined to propose such a scheme as a method for discharging rocket vehicles. Thus, for example, one would insert a probe into the exhaust plume and bias it to collect a neutralizing current to maintain zero rocket potential. This scheme does not appear to be very promising, however, because of the observations made in connection with Fig. A-7 that the circulating currents do not appreciably affect the net charging current. To test this scheme further, the test with the biased diffuser was repeated with one microammeter measuring net charging current and the other measuring diffuser line current. The results of this experiment are shown in Fig. A-10. It is noted that the net charging current to the system does not change

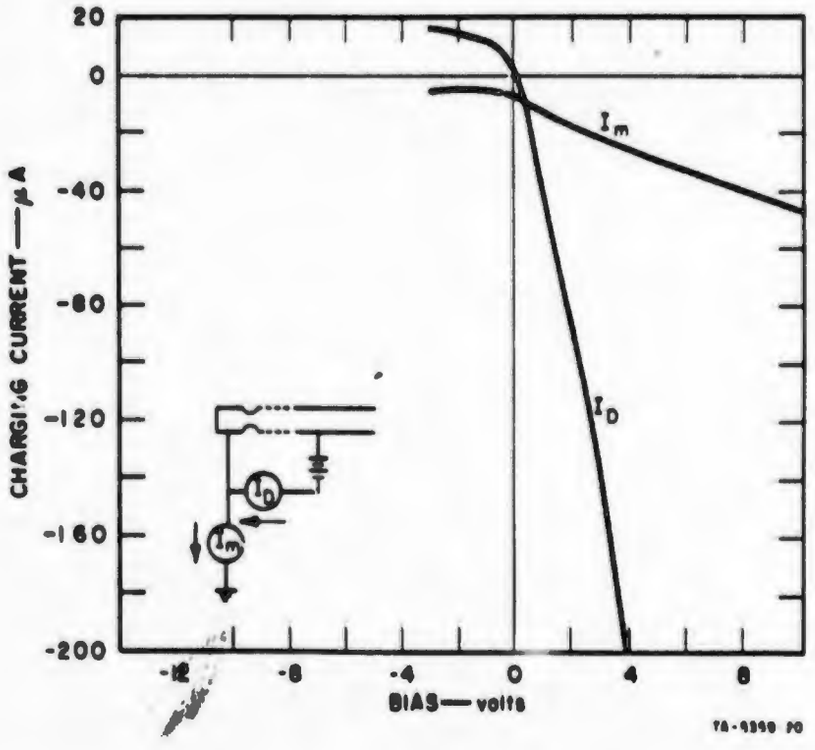

FIG. A-10 NET CHARGING CURRENT AND CIRCULATING CURRENT AS A FUNCTION OF BIAS VOLTAGE IN ETHYLENE-OXYGEN BURNER

direction even though the diffuser current changes from the saturation value in one direction to a very large value in the opposite direction. It seems probable, therefore, that the biased probe scheme for discharging rocket vehicles will be ineffective.

The experiments with the biased diffuser are also interesting because of the behavior of the circulating component of current in the vicinity of zero bias. It is noted in Figs. A-8 and A-10 that a slight change in bias voltage in this region can produce a large change in circulating current, and that the direction of current flow can be reversed with a small change in bias. It is believed that this characteristic had a bearing on the results of the static firings of the aluminized motors, in which the currents flowed in opposite directions in the two test firings. Since the exhaust of the aluminized motors is probably at least as conductive as the ethylene oxygen exhaust, a change of only a fraction of a volt in bias can reverse the direction of flow. The motor-diffuser loop undoubtedly contains some bias sources as a result of thermoelectric junctions and contact potentials. This bias can be either positive or negative, depending on the circuit components used and the manner in which they are assembled. Since the motor charging apparatus was dismantled and reassembled between the two aluminized motor firings, it is suspected that the different directions of current flow observed in the two firings was caused by different bias voltages built into the motor-diffuser loop in the two experiments.

Appendix B

MEASUREMENTS OF MOTOR POTENTIAL DURING STATIC FIRINGS

Appendix B

MEASUREMENTS OF MOTOR POTENTIAL DURING STATIC FIRINGS

The motors used in these tests were similar to those used in the earlier static firings described in Appendix A. To eliminate the effects of conducting walls or other objects in or near the exhaust, the motors were fired in an open field with the exhaust directed vertically upward. The motors were mounted on a 30-inch-square aluminum plate edged with 3-inch-diameter tubing to eliminate corona (Figs. B-1 and B-2). This plate was supported by eight 7-1/2-inch-high Teflon insulators, which in turn were supported on another 30-inch-square aluminum plate edged with 3-inch tubing. Atop the upper plate a motor holder was fabricated from smooth stock and edged with large tubing to prevent the motor housing from going into corona. Figure B-3 is a close-up of the motor holder with a motor installed. The test fixture was tested for insulation strength and corona loss by applying 150 kilovolts between the upper plate and the grounded lower plate. With this voltage applied, insulation leakage and corona loss were less than 1.0 μamp.

To measure the potential to which the motor charged the upper plate, a rotating vane electric field meter was installed in the center of the bottom plate. Since the field strength at the surface of the bottom plate is directly proportional to the potential difference between the plates, a measure of this field is a measure of the potential of the upper plate. Used in this manner, therefore, the field meter constituted a dc voltmeter of infinite impedance. The only electrical path between the motor and ground was through the air or through the 7-1/2-inch-long Teflon insulators. The field meter was provided with a synchronous detector so that polarity, as well as magnitude could be determined. The minimum motor potential detectable with the field meter was slightly less than 100 volts, and the maximum potential that could be reliably measured was 100 kilovolts. The field meter response was recorded on a moving paper recorder during the firings.

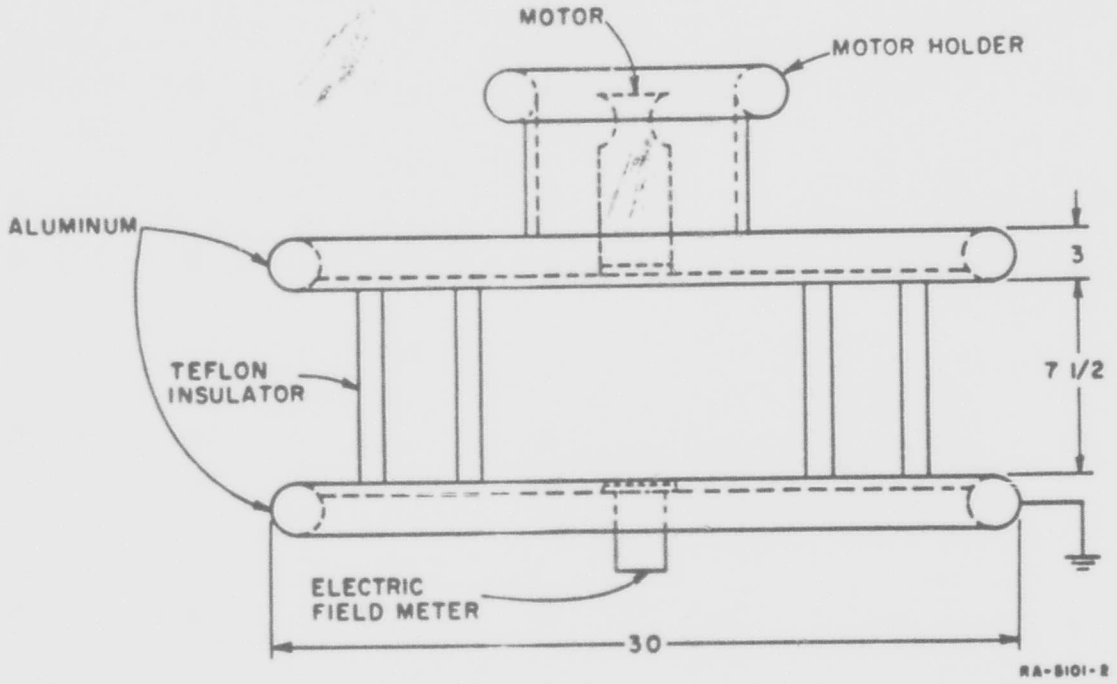

FIG. B-1 APPARATUS FOR MEASURING VEHICLE POTENTIAL IN STATIC FIRINGS

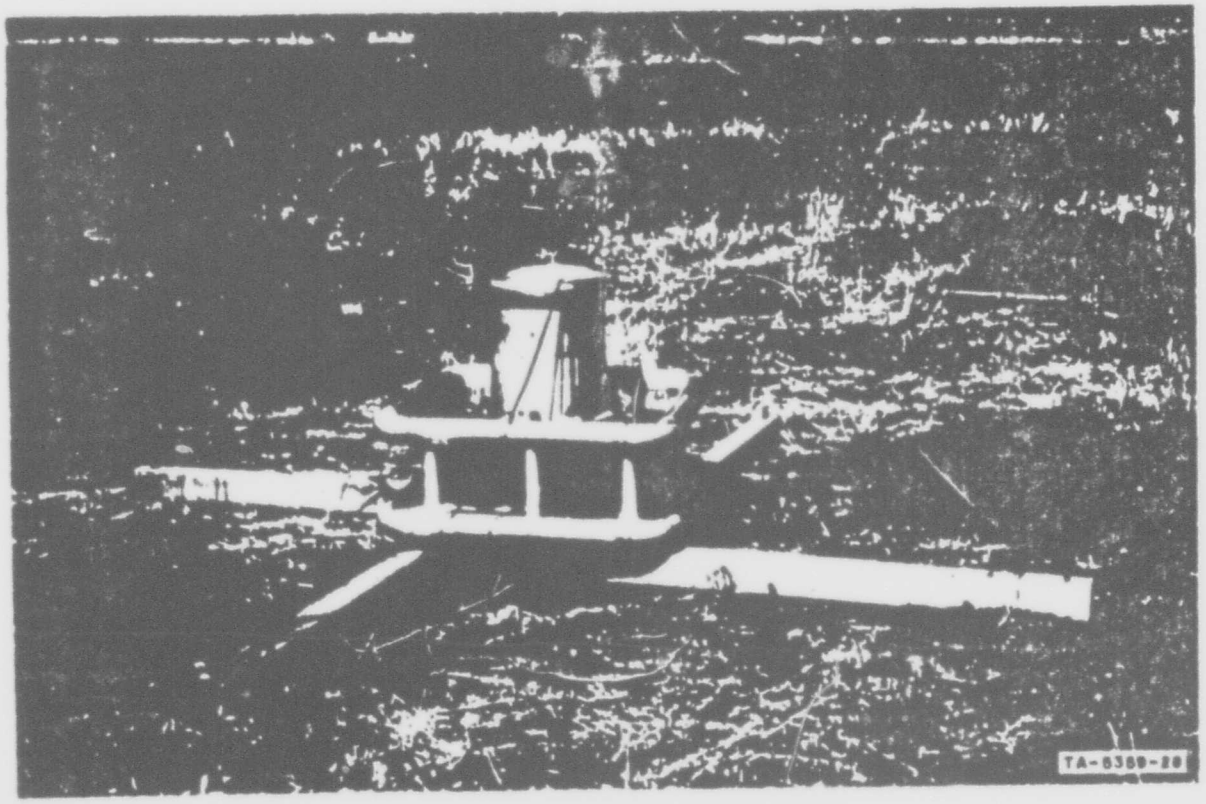

FIG. B-2 TEST APPARATUS PRIOR TO FIRING

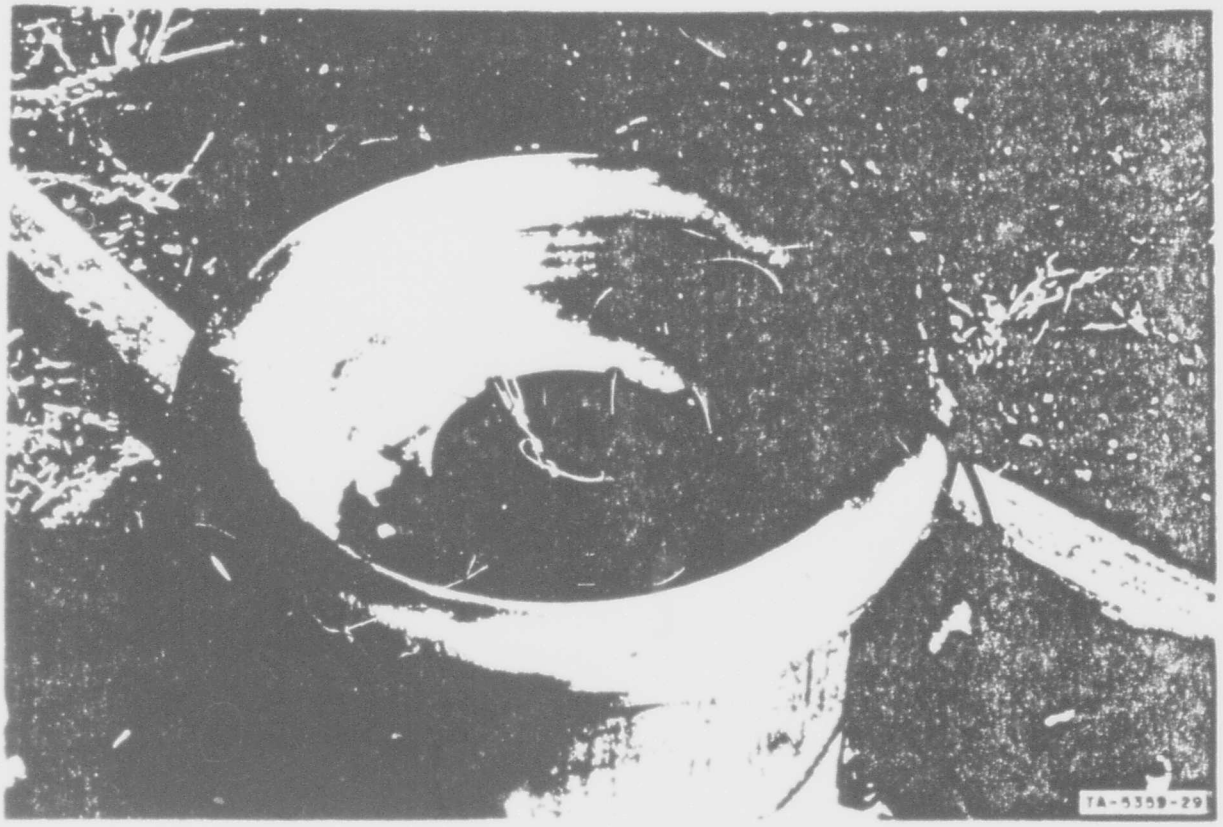

FIG. B-3 CLOSE-UP VIEW OF MOTOR INSTALLED IN TEST FIXTURE

The motors were ignited by an electric initiator inserted through the nozzle. Since the igniter leads could ground the upper plate of the test fixture if they were not removed after ignition, a special lanyard was constructed to withdraw the firing leads after ignition. The lanyard and firing leads collapsed to the ground after ignition, so that no structure was in the vicinity of the exhaust during motor burning.

A total of five 5-inch polyurethane and ammonium perchlorate motors were fired in this series of experiments. Three of these contained only a 1 percent potassium seed, and the other two contained the 1 percent potassium and 15 percent aluminum. Burning time for the motors was about 3 sec.

In the initial tests, one potassium seeded motor and one aluminized motor were fired in a test fixture as shown in Figs. B-1 and B-2. The results of these tests are shown in Fig. B-4 (a), where the potential to

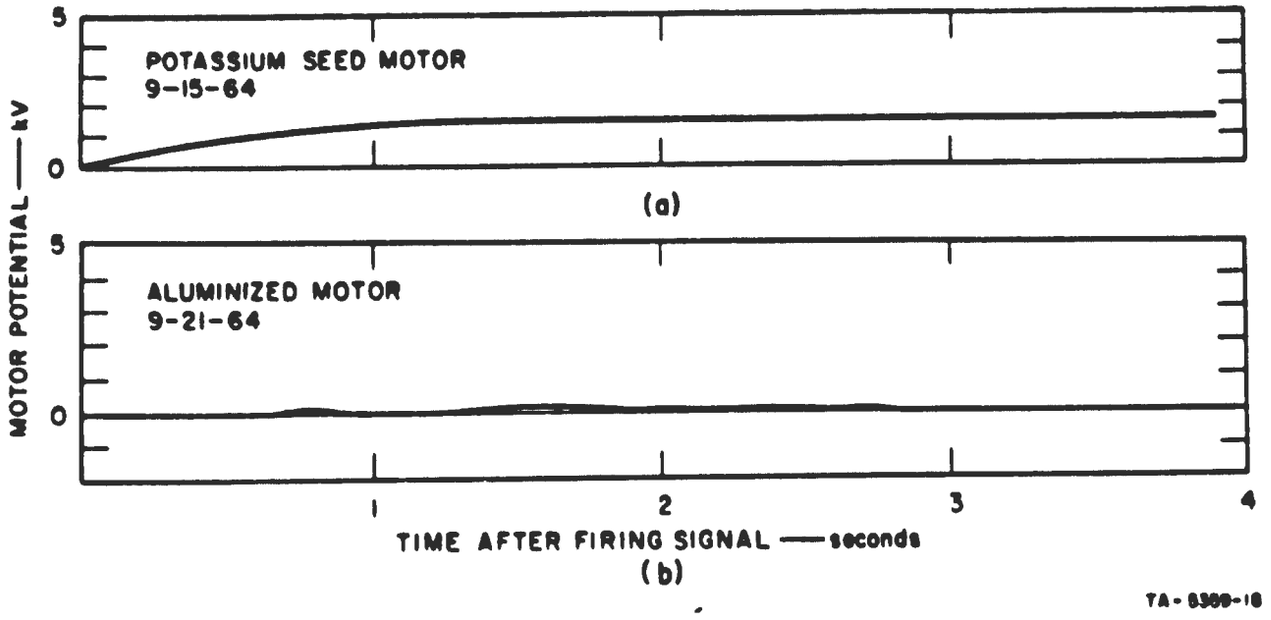

FIG. B-4 MOTOR POTENTIALS MEASURED DURING STATIC FIRING

which the motor charged the upper plate of the test fixture is plotted as a function of time. As indicated in Fig. B-4(a), the potassium seeded motor charged to slightly over one kilovolt (positive) during the first second of burning and remained at that potential. The motor apparently extinguished abruptly, since the upper plate of the test fixture remained at the 1.4 kilovolt potential for several minutes after burnout (in fact, the fixture remained charged until it was manually discharged by touching a ground wire to the upper plate) whereas on some of the subsequent tests, some of the charge was dissipated by smoke or slow post-burning combustion.

The charging characteristic shown in Fig. B-4(b) for the aluminized motor was even more surprising than that obtained for the potassium seeded motor. It had been anticipated that the ionized exhaust plume would tend to limit the potential to which the motor would charge, but it was not suspected that the potential would be limited to such low values. As the figure illustrates, the motor potential was barely detectable at the field meter sensitivity levels used in this experiment. (All of the charging characteristics shown in this section are direct reproductions from the original data recordings.) It should also be noted that the aluminized motor charged to positive potentials, as did the potassium seeded motor.

Although the potentials were much lower than had been anticipated, there appears to be a logical pattern in the ultimate potentials. Since the aluminized motor is characterized by a greater electron density in the combustion chamber and exhaust, the plume is more conductive and is a better discharger. Thus one would expect that the exhaust plume of the aluminized motor would limit the potential to a lower value, as was observed. It also appears reasonable that the scale of the motors and exhaust plume should have some effect on the potential to which the motors charge, since the effectiveness of the plume as a discharger depends on the field strength about the plume. Because the potential required to produce a given field strength about the plume is less for a slender plume than for a larger, geometrically similar plume, the potential of the smaller motor will be limited to a lower value by charge recaptured from the plume by these fields.

The remaining motors were used to perform experiments to test the electron diffusion theory of engine charging and study the effect of fields in the vicinity of the plume in discharging the motor. It was reasoned that if electron diffusion were the charging mechanism in jet engines, the same mechanism should operate within the combustion chamber of rocket engines. If the exhaust plume were highly conductive, however, the rate of capture of ions from the exhaust might be sufficient to essentially eliminate the effect of electron diffusion charging. However, if the exhaust were in a field-free region until the electrons attached to neutral molecules and some recombination occurred, the rate of capture of ions from the exhaust should be greatly reduced and the ability of the plume to discharge the motor should be considerably reduced. To provide a field-free region about the plume, the plume must be surrounded with a conductive cover so that the electrostatic field lines terminate on the cover instead of the plume.

Accordingly, a tube 2 feet in diameter and 10 feet high was fabricated from 1/4-inch mesh hardware cloth and installed over the motor mount. The hardware cloth tube prevented static fields from reaching the exhaust plume, yet allowed flow of air and exhaust gases in the exhaust region. The upper end of the tube was covered with

hardware-cloth, so that the entire visible plume was within the electrostatic shield. Corners of the shield were edged in 2-inch-diameter tubing to prevent corona loss. (No tests were conducted to determine the corona threshold voltage of the shield, but is estimated to have been greater than 100 kilovolts.)

Two motors, one with the potassium seed and one aluminized, were fired with the closed shield described above. The potentials to which the motors charged are shown in Fig. B-5. As illustrated in Fig. B-5(a) the potassium seeded motor initially charged positively, reaching a peak potential of 1.6 kilovolt. Within about 0.3 sec, however, the polarity reversed and the motor charged negatively for the remainder of the

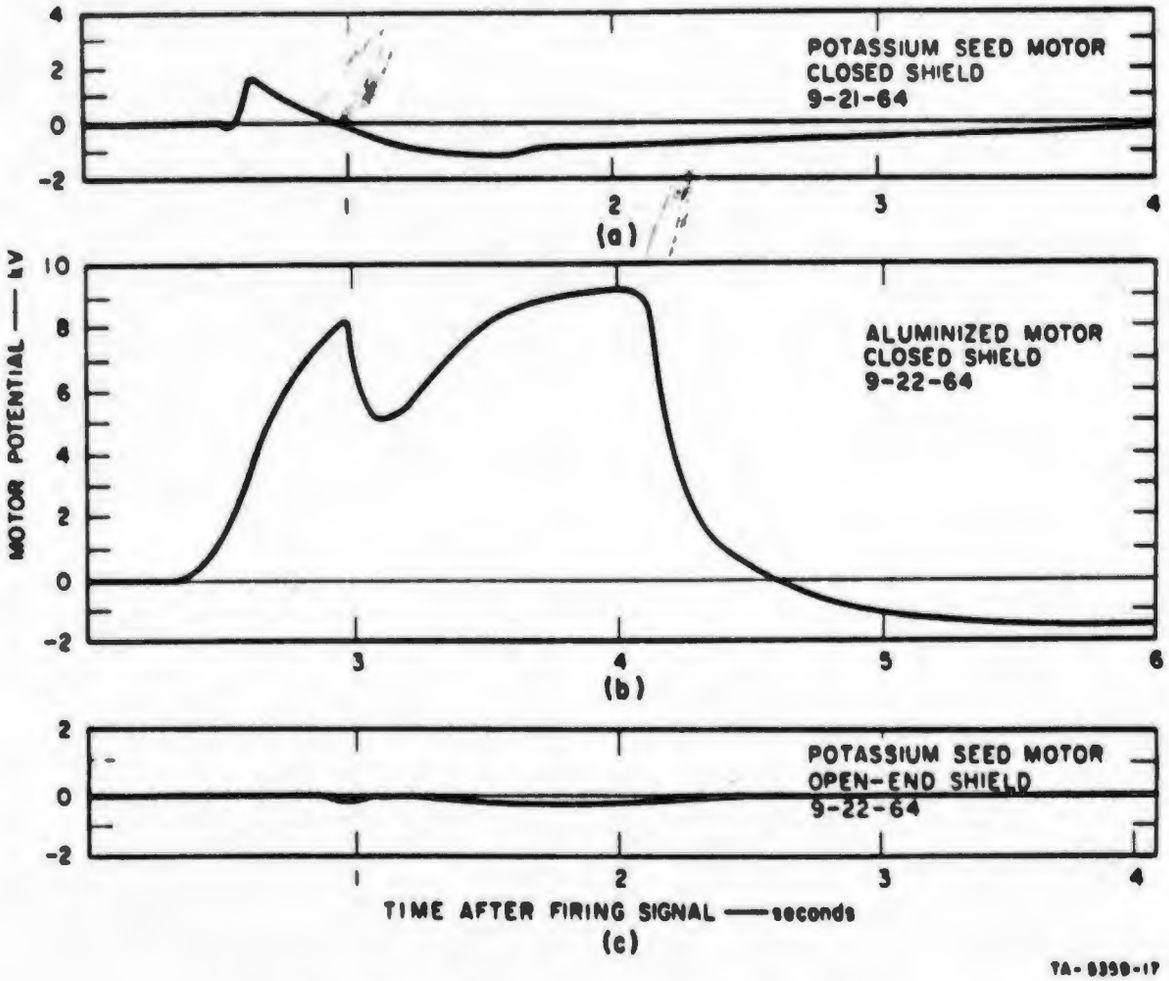

FIG. B-5 MOTOR POTENTIALS MEASURED DURING STATIC FIRING WITH ELECTROSTATIC SHIELD OVER EXHAUST PLUME

burning period, reaching a maximum negative potential of about 1.2 kilovolts. The charging characteristics shown in Fig. B-5(b) for the aluminized motor are quite different, however; the aluminized motor charged positively for most of the burning period, reaching a maximum potential of slightly over 9 kilovolts. Before burnout, the polarity reversed and the motor charged to a negative potential of 1.5 kilovolts.

Before firing the third motor in the shielded configuration, the hardware cloth end closure at the top of the shield was removed, leaving only the cylindrical walls of the shield. The sides of the plume were thus shielded from electrostatic fields, but because of fringing at the upper end of the shield, it may have been possible for some field lines to terminate on the end of the plume. A potassium seeded motor was fired in this open-end shield configuration to produce the charging characteristics shown in Fig. B-5(c). The motor charged negatively throughout the burning period, but the maximum potential attained only about 260 volts.

The tests with the closed shields suggest that the discharging capability of the plume is reduced somewhat if the highly conductive part of the plume is shielded from the electrostatic fields of the charged motor (Section III-C). This indication is particularly strong in the case of the aluminized motors. The unshielded motor of Fig. B-4(b) charged to only about 200 volts, while the shielded motor of Fig. B-5(b) charged to over 9 kilovolts. The effect of shielding the plume is less striking in the cases of the nonaluminized motors, but even here, the closed shield appears to have enhanced the maximum motor potential slightly.

Appendix C

FIELD METER CIRCUIT DIAGRAM

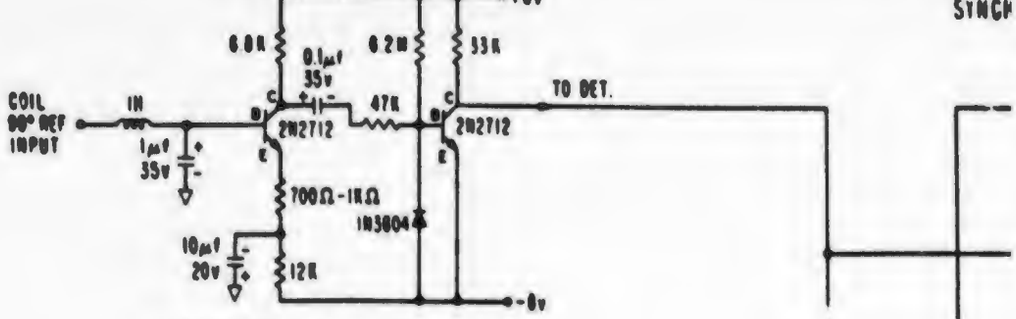

90° REFERENCE AMPLIFIER

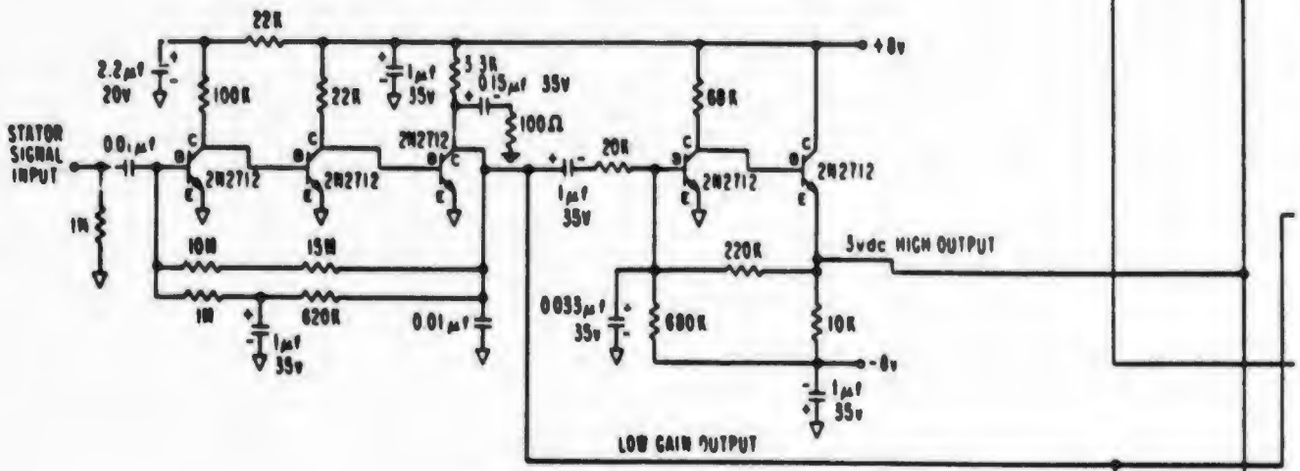

SIGNAL AMPLIFIER

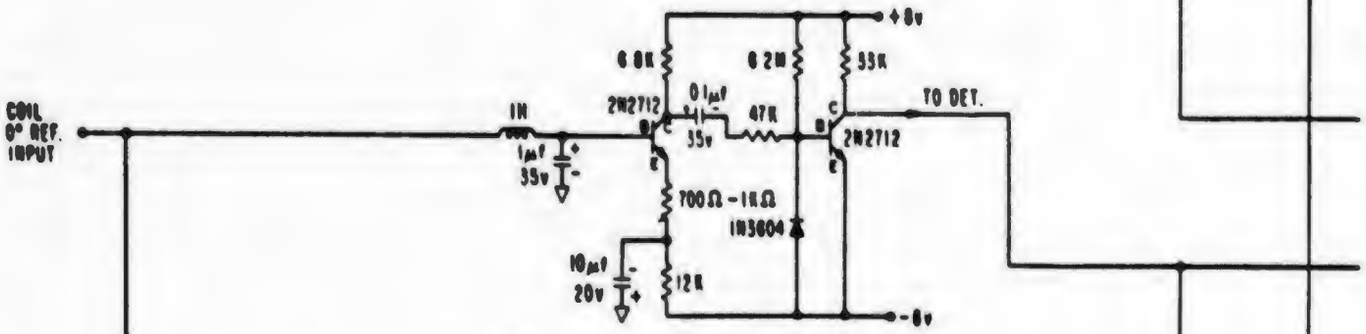

0° REFERENCE AMPLIFIER

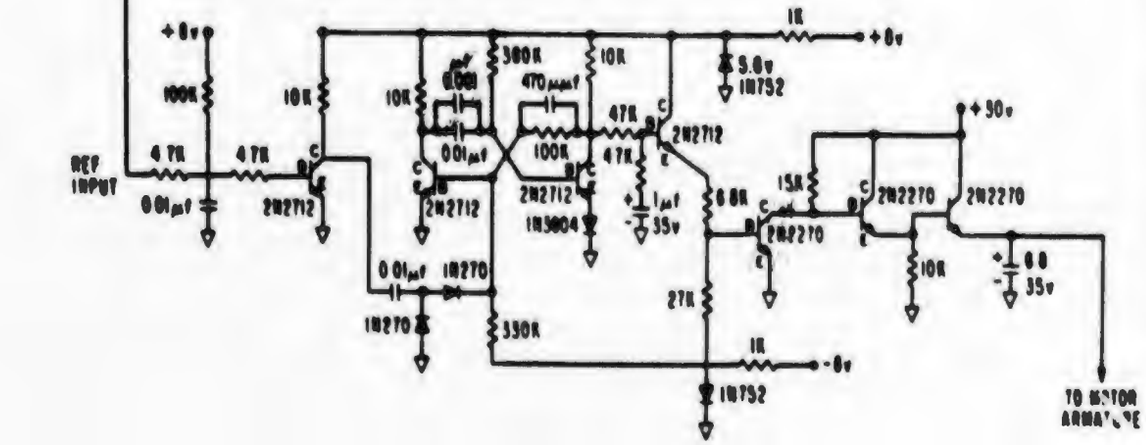

MOTOR SPEED CONTROL

A

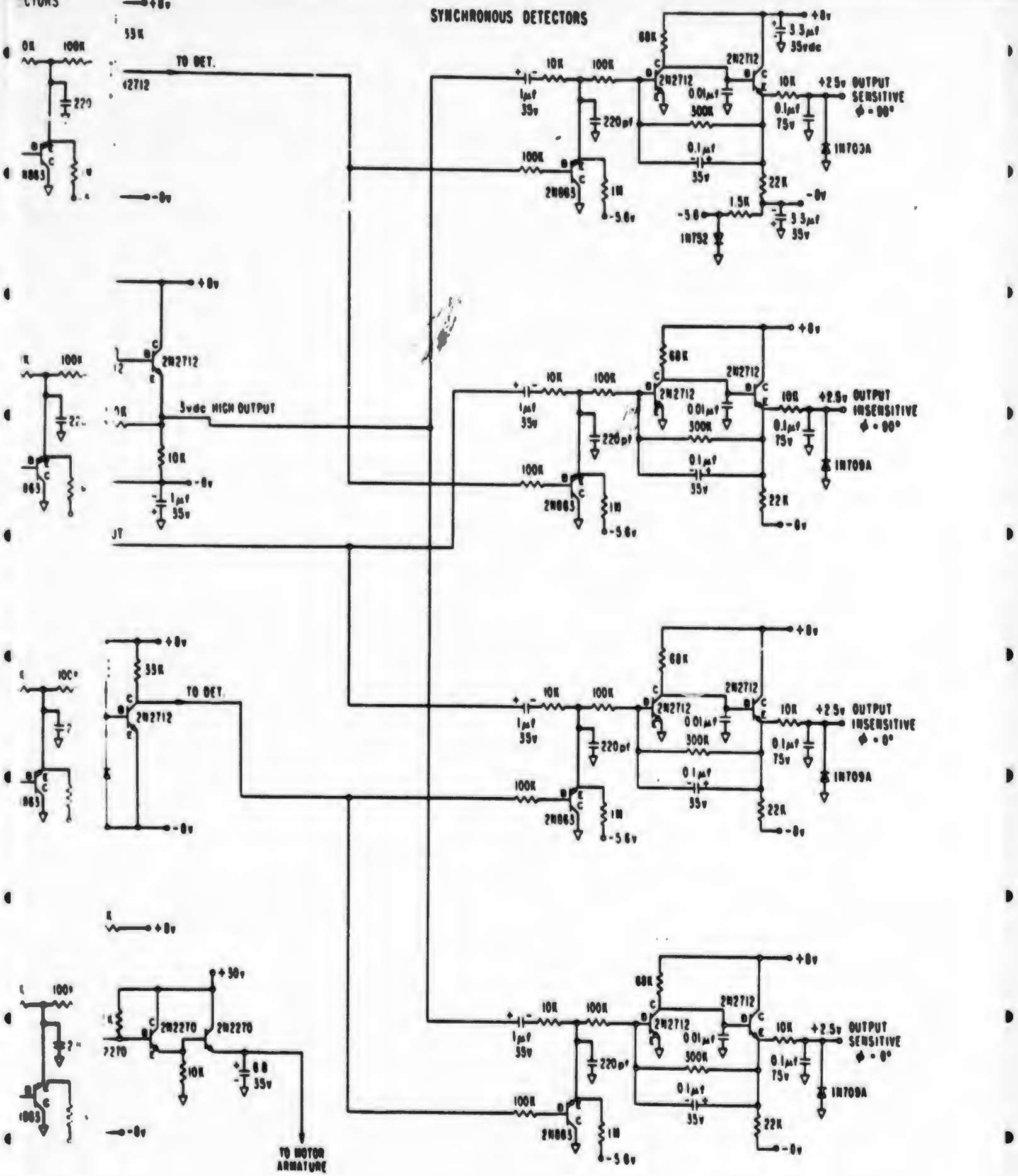

TD-8388-16

FIELD METER CIRCUIT DIAGRAM

REFERENCES

1. J. E. Nanevicz, et al., "Development and Testing of Techniques for Precipitation Static Interference Reduction," Final Report, Contract AF 33(616)-6561, SRI Project 2848, Stanford Research Institute, Menlo Park, California (January 1962).

2. R. L. Tanner and J. E. Nanevicz, "Precipitation Charging and Corona-Generated Interference in Aircraft," Technical Report 73, SRI Project 2494, Contract AF 19(604)-3458, Stanford Research Institute, Menlo Park, California (April 1961).

3. E. F. Vance, L. B. Seely, and J. E. Nanevicz, "Effects of Vehicle Electrification on Apollo Electro-Explosive Devices," Final Report, Contract NAS 9-3154, SRI Project 5101, Stanford Research Institute, Menlo Park, California (December 1964).

4. P. Molmud, "Frictional Electricity in Missile Systems," J. Am. Roc. Soc., pp. 73-74 (January 1959).

5. J. E. Nanevicz, et al., "Low-Altitude, Long-Range, All-Weather Vehicle Interference Investigation," AFAL-TR-65-239, Part I, Prepared for Air Force Avionics Laboratory, Wright-Patterson Air Force Base, Ohio (December 1965).

6. T. L. Harlor, A. R. Jordan and D. G. Murcray, "Development of Aircraft Discharge Methods," Final Report, Contract No. AF 33(616)-157, Denver Research Institute, University of Denver, Denver, Colorado (April 1956).

7. E. L. Capener, et al., "Study of Microwave and Visible Light Wave Transmission through Solid Propellent Exhaust Gases," Final Report, SRI Project PRU-4177, Contract NAS7-179, Stanford Research Institute, Menlo Park, California (April 1964).

8. E. L. Capener, et al., "Studies on Ionization Phenomena Associated with Solid Propellant Rockets," Paper No. 65-182 Presented at the AIAA Sixth Solid Propellant Conference, Washington, D.C. (February 1965).

9. J. C. Axtell, "Preliminary Minuteman Electrostatic Charge Studies," Model No. WS-133a, Contract AF 04(647)-580, The Boeing Company, Seattle, Washington (1963).

10. R. M. Fristrom, F. A. Oyhus and G. M. Albrecht, "Charge Buildup on Solid Rockets as a Flame Burst Mechanism," ARS Journal (November 1962), pp. 1729-1730.

11. D. McIver, Langley Research Center, Hampton, Virginia. Private Communication (September 1964).

12. H. Leuder, "Investigation of Electrostatic Charging and Radio Interference on DS-1400 X Glide Bomb, "Translation Report No. F-TS-1824-RE, Headquarters, Air Materiel Command, Wright Field, Dayton, Ohio (Translation released June 1947).

UNCLASSIFIED

Security Classification

DOCUMENT CONTROL DATA - R&D

(Security classification of title, body of abstract and indexing annotation must be entered when the overall report is classified)

1 ORIGINATING ACTIVITY (Corporate author)

Stanford Research Institute
Menlo Park, California

2a. REPORT SECURITY CLASSIFICATION
UNCLASSIFIED

2b GROUP

3 REPORT TITLE

ROCKET MOTOR CHARGING EXPERIMENTS

4 DESCRIPTIVE NOTES (Type of report and inclusive dates)

Scientific Interim Report 2

5 AUTHOR(S) (Last name, first name, initial)

[illegible], E. F. Namenwirz, J. E.

6 REPORT DATE	7a. TOTAL NO. OF PAGES	7b. NO. OF REFS
June 1966	110	18

8a CONTRACT OR GRANT NO. AF 19(628)-4800	9a. ORIGINATOR'S REPORT NUMBER(S)
b PROJECT NO. Task 4600.10	SRI Project 5359
c 62105304	9b. OTHER REPORT NO(S) (Any other numbers that may be assigned this report)
d [illegible]	AFCRL-66-497

10 AVAILABILITY/LIMITATION NOTICES

Distribution of this document is unlimited.

11. SUPPLEMENTARY NOTES	12. SPONSORING MILITARY ACTIVITY
	Hq., AFCRL, OAR (CRD) United States Air Force L. G. Hanscom Field, Bedford, Massachusetts

13 ABSTRACT

A study of the effect of rocket engines on electrostatic charge accumulation was made. Experiments were conducted to measure short-circuit charging current and open-circuit voltage produced by 5-inch solid-fuel rocket motors during static firings at sea level. Experiments were also performed with an ethylene-oxygen burner at reduced pressures (14 mmHg). The results of these experiments are presented and compared to the published results of related experiments.

Two Nike-Cajun sounding rockets were equipped with electric field meters to measure the vehicle potential throughout the rocket flight. The field meters indicated that the maximum vehicle potential was 26-to 40 kilovolts during first-stage burning at about 3 kilometers and about 2 kilovolts during second-stage burning at about 12 kilometers. At high altitudes, the field meter on the first Nike-Cajun responded to ionization present in the ionosphere and enhanced by a primary experiment. This undesired response was successfully separated from the true field response in the field meter system designed for the second Nike-Cajun experiment. It was, therefore, possible to conclude that the potential of the second vehicle was less than 1 kilovolt at altitudes above 60 kilometers (in the ionosphere).

DD FORM 1 JAN 64 1473

UNCLASSIFIED

Security Classification

UNCLASSIFIED

Security Classification

14 KEY WORDS	LINK A		LINK B		LINK C	
	ROLE	WT	ROLE	WT	ROLE	WT
rocket engines						
rocket charging						
charging current						
electrostatic charging						
rocket potential						
electrostatic field measurement						
rocket experiments						
flight test measurements						

INSTRUCTIONS

1. **ORIGINATING ACTIVITY:** Enter the name and address of the contractor, subcontractor, grantee, Department of Defense activity or other organization *(corporate author)* issuing the report.

2a. **REPORT SECURITY CLASSIFICATION:** Enter the overall security classification of the report. Indicate whether "Restricted Data" is included. Marking is to be in accordance with appropriate security regulations.

2b. **GROUP:** Automatic downgrading is specified in DoD Directive 5200.10 and Armed Forces Industrial Manual. Enter the group number. Also, when applicable, show that optional markings have been used for Group 3 and Group 4 as authorized.

3. **REPORT TITLE:** Enter the complete report title in all capital letters. Titles in all cases should be unclassified. If a meaningful title cannot be selected without classification, show title classification in all capitals in parenthesis immediately following the title.

4. **DESCRIPTIVE NOTES:** If appropriate, enter the type of report, e.g., interim, progress, summary, annual, or final. Give the inclusive dates when a specific reporting period is covered.

5. **AUTHOR(S):** Enter the name(s) of author(s) as shown on or in the report. Enter last name, first name, middle initial. If military, show rank and branch of service. The name of the principal author is an absolute minimum requirement.

6. **REPORT DATE:** Enter the date of the report as day, month, year, or month, year. If more than one date appears on the report, use date of publication.

7a. **TOTAL NUMBER OF PAGES:** The total page count should follow normal pagination procedures, i.e., enter the number of pages containing information.

7b. **NUMBER OF REFERENCES:** Enter the total number of references cited in the report.

8a. **CONTRACT OR GRANT NUMBER:** If appropriate, enter the applicable number of the contract or grant under which the report was written.

8b, 8c, & 8d. **PROJECT NUMBER:** Enter the appropriate military department identification, such as project number, subproject number, system numbers, task number, etc.

9a. **ORIGINATOR'S REPORT NUMBER(S):** Enter the official report number by which the document will be identified and controlled by the originating activity. This number must be unique to this report.

9b. **OTHER REPORT NUMBER(S):** If the report has been assigned any other report numbers *(either by the originator or by the sponsor)*, also enter this number(s).

10. **AVAILABILITY/LIMITATION NOTICES:** Enter any limitations on further dissemination of the report, other than those imposed by security classification, using standard statements such as:

(1) "Qualified requesters may obtain copies of this report from DDC."

(2) "Foreign announcement and dissemination of this report by DDC is not authorized."

(3) "U. S. Government agencies may obtain copies of this report directly from DDC. Other qualified DDC users shall request through _____."

(4) "U. S. military agencies may obtain copies of this report directly from DDC. Other qualified users shall request through _____."

(5) "All distribution of this report is controlled. Qualified DDC users shall request through _____."

If the report has been furnished to the Office of Technical Services, Department of Commerce, for sale to the public, indicate this fact and enter the price, if known.

11. **SUPPLEMENTARY NOTES:** Use for additional explanatory notes.

12. **SPONSORING MILITARY ACTIVITY:** Enter the name of the departmental project office or laboratory sponsoring *(paying for)* the research and development. Include address.

13. **ABSTRACT:** Enter an abstract giving a brief and factual summary of the document indicative of the report, even though it may also appear elsewhere in the body of the technical report. If additional space is required, a continuation sheet shall be attached.

It is highly desirable that the abstract of classified reports be unclassified. Each paragraph of the abstract shall end with an indication of the military security classification of the information in the paragraph, represented as *(TS), (S), (C), or (U)*.

There is no limitation on the length of the abstract. However, the suggested length is from 150 to 225 words.

14. **KEY WORDS:** Key words are technically meaningful terms or short phrases that characterize a report and may be used as index entries for cataloging the report. Key words must be selected so that no security classification is required. Identifiers, such as equipment model designation, trade name, military project code name, geographic location, may be used as key words but will be followed by an indication of technical context. The assignment of links, roles, and weights is optional.

DD FORM 1 JAN 64 1473 (BACK)

UNCLASSIFIED

Security Classification